(12) INTERNATIONAL APPLICATION PUBLISHED UNDER THE PATENT COOPERATION TREATY (PCT)

(19) World Intellectual Property Organization
International Bureau

(43) International Publication Date
11 August 2016 (11.08.2016)

WIPO | PCT

(10) International Publication Number
WO 2016/126314 A1

(51) International Patent Classification:
G01N 21/65 (2006.01) *G01N 33/50* (2006.01)
A61B 5/00 (2006.01)

(21) International Application Number:
PCT/US2015/063801

(22) International Filing Date:
3 December 2015 (03.12.2015)

(25) Filing Language: English

(26) Publication Language: English

(30) Priority Data:
62/111,544 3 February 2015 (03.02.2015) US

(71) Applicant: **NORTHEASTERN UNIVERSITY** [US/US]; 360 Huntington Avenue, 900RP, Boston, MA 02115 (US).

(72) Inventor: **CHAMPION, Paul, M.**; 65 Sunset Rock Road, Andover, MA 01810 (US).

(74) Agents: **SOLOMON, Mark, B.** et al.; Hamilton, Brook, Smith & Reynolds, P.C., 530 Virginia Rd, P.O. Box 9133, Concord, MA 01742-9133 (US).

(81) Designated States *(unless otherwise indicated, for every kind of national protection available)*: AE, AG, AL, AM, AO, AT, AU, AZ, BA, BB, BG, BH, BN, BR, BW, BY, BZ, CA, CH, CL, CN, CO, CR, CU, CZ, DE, DK, DM, DO, DZ, EC, EE, EG, ES, FI, GB, GD, GE, GH, GM, GT, HN, HR, HU, ID, IL, IN, IR, IS, JP, KE, KG, KN, KP, KR, KZ, LA, LC, LK, LR, LS, LU, LY, MA, MD, ME, MG, MK, MN, MW, MX, MY, MZ, NA, NG, NI, NO, NZ, OM, PA, PE, PG, PH, PL, PT, QA, RO, RS, RU, RW, SA, SC, SD, SE, SG, SK, SL, SM, ST, SV, SY, TH, TJ, TM, TN, TR, TT, TZ, UA, UG, US, UZ, VC, VN, ZA, ZM, ZW.

(84) Designated States *(unless otherwise indicated, for every kind of regional protection available)*: ARIPO (BW, GH, GM, KE, LR, LS, MW, MZ, NA, RW, SD, SL, ST, SZ, TZ, UG, ZM, ZW), Eurasian (AM, AZ, BY, KG, KZ, RU, TJ, TM), European (AL, AT, BE, BG, CH, CY, CZ, DE, DK, EE, ES, FI, FR, GB, GR, HR, HU, IE, IS, IT, LT, LU, LV, MC, MK, MT, NL, NO, PL, PT, RO, RS, SE, SI, SK, SM, TR), OAPI (BF, BJ, CF, CG, CI, CM, GA, GN, GQ, GW, KM, ML, MR, NE, SN, TD, TG).

Declarations under Rule 4.17:

— *of inventorship (Rule 4.17(iv))*

Published:

— *with international search report (Art. 21(3))*

— *before the expiration of the time limit for amending the claims and to be republished in the event of receipt of amendments (Rule 48.2(h))*

(54) Title: METHODS AND SYSTEMS FOR DETECTING APOPTOSIS

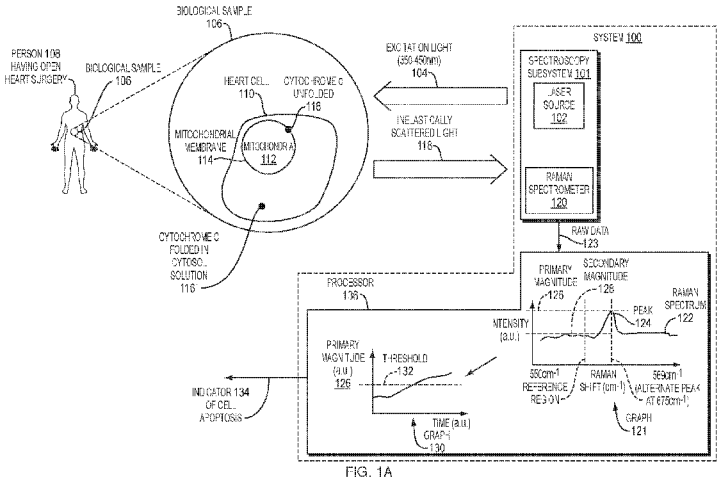

FIG. 1A

(57) Abstract: A system and corresponding method for detecting cell apoptosis includes a laser source configured to apply an incident excitation wavelength to a biological sample. The wavelength is in resonance with a heme group. A detector is configured to detect inelastic light scattering resulting from a vibrational mode of cytochrome *b* or cytochrome *c*. A processor is configured to monitor the biological sample based on the light scattering for a change of cytochrome *b* state or an increase in cytochrome *c* in a folded state in solution relative to cytochrome *c* in an unfolded state in a mitochondrial membrane to detect initiation of apoptosis. The laser source and detector can be mounted within a patch and applied to a person. Embodiments provide for convenient monitoring of tissue health, determination of efficacy of stimulants for inducing apoptosis in cells in research, and early detection of cell apoptosis.

WO 2016/126314 A1

METHODS AND SYSTEMS FOR DETECTING APOPTOSIS

RELATED APPLICATIONS

[0001] This application claims the benefit of U.S. Provisional Application No. 62/111,544, filed on February 3, 2015. The entire teachings of the above application are incorporated herein by reference.

GOVERNMENT SUPPORT

[0002] This invention was made with government support under NIH DK35090 (P.M.C.), GM57563 (H. W.), and NSF MCB 0211816 (P.M.C.). The government has certain rights in the invention.

BACKGROUND

[0003] Raman spectroscopy has been used as a tool to investigate various types of biological cells. Resonance Raman spectroscopy can be particularly helpful because it can lead to scattering signals that are much stronger and easier to detect. Cytochrome *c* forms part of an electron transport mechanism in mitochondria. Cytochrome *c* has a different structural form within the mitochondria of cells than when it falls out of (is released from) the mitochondria. The falling out of cytochrome *c* from mitochondrial membranes of cells into solution outside the mitochondria is known to be a part of the process of programmed cell death through apoptosis.

SUMMARY

[0004] Investigations of Raman scattering from cytochrome *c* have not produced a spectral difference that can be used, as a practical matter, to distinguish between cytochrome *c* in mitochondrial membranes and cytochrome *c* in solution. A specific novel feature of some embodiment devices and methods is use of a vibrational mode near 570 cm^{-1} in the Raman spectrum of cytochrome *c* that appears when cytochrome *c* folds tightly in solution and ruffles a heme group in the cytochrome *c*. This ruffling turns on the selection rules that activate a variety of out-of-plane heme vibrational modes. In contrast to the solution state, these modes are absent when cytochrome *c* binds to the mitochondrial membrane. A particular advantage of embodiments is that Raman spectroscopy is a label-free method of

detecting apoptosis in live cells or tissues. In particular, resonance Raman spectroscopy, with monitoring of a vibrational mode near 570 cm^{-1}, can be used to distinguish readily between cytochrome *c* in solution and cytochrome *c* in mitochondrial membranes of cells. This leads to a sensitive method for early detection of apoptosis. In some embodiments, systems and methods can be used advantageously to monitor cells in patients for surgical or post-operative purposes, for example. Furthermore, in some embodiments, the systems and methods are useful as research tools, where propensity for specific stimulants for producing cell apoptosis can be evaluated. This can have potential use in cancer therapy, for example.

[0005] In one embodiment, a system for monitoring for cell apoptosis includes a patch configured to be applied to a person. A laser source in the patch is configured to apply an incident excitation wavelength to a biological sample, with the biological sample from, or being part of, the person. A detector in the patch is configured to detect inelastic light scattering from the biological sample, where the light scattering is caused by the incident excitation wavelength. The system also includes a processor configured to monitor the state of the biological sample based on the light scattering. The patch can be in the form of a module strapped to or otherwise attached to or worn by a person.

[0006] The laser source can be configured to apply the incident excitation wavelength in a resonance wavelength band for a heme group of cytochrome *c* in the biological sample. Furthermore, in some embodiments, the detector is configured to detect inelastic light scattering with a Raman shift at about 569 cm^{-1}, with the inelastic light scattering resulting from a vibrational scattering mode of cytochrome *c*, resulting in the Raman shift at about 569 cm^{-1}.

[0007] The processor can be further configured to monitor the biological sample based on the light scattering at the inelastic Raman shift of about 569 cm^{-1}, for an increase in cytochrome *c* in a folded state in solution relative to cytochrome *c* in an unfolded state in a mitochondrial membrane of a cell in the biological sample.

[0008] The detector can also be configured to detect inelastic light scattering with a Raman shift at about 675 cm^{-1}, the inelastic light scattering resulting from a vibrational scattering mode of cytochrome *b*, resulting in the Raman shift at about 675 cm^{-1}. The processor can also be configured to monitor the state of biological sample, based on light scattering at an inelastic Raman shift of about 675 cm^{-1}, for a change of state of cytochrome *b* in solution to a physically altered state relative to cytochrome *b* in a mitochondrial membrane

of a cell to detect initiation of apoptosis of the cell in the biological sample. The monitoring can be used to detect initiation of apoptosis of the cell in the biological sample.

[0009] In another embodiment, a system and corresponding method for detecting cell apoptosis includes a laser source configured to apply an incident excitation wavelength to a biological sample, the incident excitation wavelength in a resonance wavelength band for a heme group of cytochrome *c*. The resonance wavelength band can be an electronic resonance. The system also includes a detector configured to detect inelastic light scattering with a Raman shift at about 569 cm^{-1}. The inelastic light scattering results from a vibrational scattering mode of the cytochrome *c*. The system further includes a processor configured to monitor the biological sample based on the light scattering in the inelastic Raman shift at about 569 cm^{-1}. An increase in this light scattering can indicate an increase in cytochrome *c* in a folded state in solution relative to cytochrome *c* in an unfolded state in a mitochondrial membrane of a cell and can be used to detect initiation of apoptosis of the cell in the biological sample.

[0010] The laser source and detector can be mounted within a patch configured to be applied to a person. The system can include an optical fiber configured to deliver scattered light from the biological sample to the detector. The processor can be located remotely from the laser source and detector, and the processor can be further configured to monitor using signals received from the detector via a signal path.

[0011] In still another embodiment, a method and corresponding system for monitoring for apoptosis in the biological sample includes applying an incident excitation wavelength to the biological sample, where the incident excitation wavelength is in a resonance wavelength band for a heme group of cytochrome *c*. The method also includes detecting inelastic light scattering with a Raman shift at about 569 cm^{-1}. The inelastic light scattering results from a vibrational scattering mode of cytochrome *c*, resulting in the Raman shift at about 569 cm^{-1}. The method also includes monitoring the biological sample, based on the light scattering in the inelastic Raman shift at about 569 cm^{-1}, to monitor an increase in cytochrome *c* in a folded state in solution relative to cytochrome *c* in an unfolded state in the mitochondrial membrane of a cell. This can be used to detect initiation of apoptosis of the cell in the biological sample.

[0012] Applying the incident excitation wavelength in a resonance wavelength band can include using a wavelength band of about 340-450 nm. The method can further include

detecting inelastic light scattering with a Raman shift in a reference scattering region of the cytochrome *c*. A scattering strength of the reference scattering can remain substantially constant with increasing cytochrome *c* in solution. Detecting the inelastic light scattering with the Raman shift at about 569 cm^{-1} and in the reference scattering region can include using respective detectors to monitor relative strengths of the Raman shift at about 569 cm^{-1} and the Raman shift in the reference scattering region.

[0013] Applying the incident excitation wavelength or detecting the inelastic light scattering can include using a fiber light guide. Applying the incident excitation wavelength can include using modulated light, and detecting the inelastic light scattering can include detecting the inelastically scattered light synchronously with the incident modulated light. In some embodiments, the cell can be a heart cell. In some embodiments, the cell can be a cancer cell. In some embodiments, the cell can be an organ transplant cell. The biological sample can be an *in vivo* sample, *ex vivo* sample, or *in vitro* sample.

[0014] The method can also include using the increase in cytochrome *c* in the folded state in solution as an indicator of poor mitochondrial health in the cell. Furthermore, the method can include calibrating a spectroscopic device used to monitor the biological sample by facilitating a process of cell apoptosis.

[0015] In yet another embodiment, a method of detecting a stimulus' efficacy for inducing apoptosis in a test cell that has been exposed to the stimulus can include determining a magnitude of a primary scattering signal at a first Raman shift that represents a vibrational scattering mode of cytochrome *c* in a folded state. The method also includes determining the efficacy as a function of the magnitude of the primary scattering signal compared to a magnitude of a secondary scattering signal at a second Raman shift for a reference measurement. The magnitudes of the primary and secondary scattering signals can be determined simultaneously.

[0016] The method can further include receiving the magnitude of the primary scattering signal in the form of data, transmitted across a network communications path, at a server. The method can also include transmitting, from the server, a representation of the efficacy via the network communications path. The method can also include receiving the magnitude of the primary scattering signal in the form of data at a processor and outputting, by the processor, a representation of the efficacy. The method can include determining the efficacy of at least two stimuli for inducing apoptosis in cells that have each been exposed to a

respective stimulus and selecting a stimulus from the at least two stimuli based on a comparison of the efficacy of the stimuli.

[0017] Determining the efficacy can include analyzing a ratio of the magnitudes of the primary and secondary scattering signals. The magnitude of the primary or secondary scattering signal can be represented by an amplitude signal of the primary or secondary scattering signal, respectively.

[0018] In a further embodiment, a method of monitoring for apoptosis in a biological sample includes applying an incident excitation wavelength to the biological sample, the incident excitation wavelength being in a resonance wavelength band for a heme group of cytochrome *b*. The method also includes detecting inelastic light scattering with a Raman shift at about 675 cm^{-1}, the inelastic light scattering resulting from a vibrational scattering mode of cytochrome *b*, resulting in the Raman shift at about 675 cm^{-1}. The method further includes monitoring the biological sample, based on the light scattering with the inelastic Raman shift at about 675 cm^{-1}, for a change of physical state of cytochrome *b* in solution relative to cytochrome *b* in a mitochondrial membrane of a cell. The monitoring can be used to detect initiation of apoptosis of the cell in the biological sample.

[0019] The method can also include detecting inelastic light scattering with a Raman shift in a reference scattering region of the cytochrome *b*. A scattering strength of the reference scattering can remain substantially constant with respect to the change of state of cytochrome *b* in solution to a physically altered state relative to cytochrome *b* in the mitochondria. A Raman shift in a reference scattering region can include a background spectral region expected to remain substantially constant with respect to a change in physical state of cytochrome *b* that leads to a change in inelastic light scattering with the Raman shift at about 675 cm^{-1}. A reference region may also include a different Raman peak in a different spectral region than the Raman peak at 675 cm^{-1}. The different Raman peak can have a scattering intensity that varies inversely relative to the changes in the Raman peak at 675 cm^{-1}.

[0020] Detecting inelastic light scattering with the Raman shift at about 675 cm^{-1} and in the reference scattering region can include using respective detectors to monitor relative strengths of the Raman shift at about 675 cm^{-1} and the Raman shift in the reference scattering region. The reference scattering region can include a spectral region for a second Raman peak or a substantially constant background spectral region.

[0021] In a further embodiment, a system for detecting cell apoptosis includes a laser source configured to apply an incident excitation wavelength to a biological sample, the incident excitation wavelength in a resonance wavelength band for a heme group of cytochrome *b*. The system also includes a detector configured to detect inelastic light scattering with a Raman shift at about 675 cm^{-1}, the inelastic light scattering resulting from a vibrational scattering mode of the cytochrome *b*. A processor of the system is configured to monitor the biological sample, based on the light scattering in the inelastic Raman shift at about 675 cm^{-1}, for a change of physical state of cytochrome *b* in solution relative to cytochrome *b* in a mitochondrial membrane of a cell to detect initiation of apoptosis of the cell in the biological sample.

[0022] In yet a further embodiment, a method of detecting a stimulus' efficacy for inducing apoptosis in a test cell that has been exposed to the stimulus includes determining a magnitude of a primary scattering signal at a Raman shift that represents a vibrational scattering mode of cytochrome *b*. The method also includes determining the efficacy as a function of the magnitude of the primary scattering signal compared to a magnitude of a secondary scattering signal at a second Raman shift for a reference measurement.

[0023] In still a further embodiment, a method of detecting a stimulus' efficacy for inducing apoptosis in a test cell that has been exposed to the stimulus includes determining a test magnitude of a scattering signal at a Raman shift that represents a vibrational scattering mode of cytochrome *c* in a folded state, or change in physical state of cytochrome *b* to a physically altered state, from a test cell that has been exposed to a stimulus. The method also includes determining the stimulus' efficacy as a function of the test magnitude compared to a control magnitude of a scattering signal at the Raman shift that represents the vibrational scattering mode of cytochrome *c* in the folded state from a control cell that has not been exposed to the stimulus.

[0024] The test magnitude and control magnitude can be determined simultaneously. Determining the stimulus' efficacy can include analyzing a ratio of the magnitudes of the scattering signals from the test and control cells.

BRIEF DESCRIPTION OF THE DRAWINGS

[0025] The foregoing will be apparent from the following more particular description of example embodiments of the invention, as illustrated in the accompanying drawings in which

like reference characters refer to the same parts throughout the different views. The drawings are not necessarily to scale, emphasis instead being placed upon illustrating embodiments of the present invention.

[0026] FIG. 1A is a schematic diagram of a system for detecting cell apoptosis.

[0027] FIG. 1B is a more detailed schematic diagram of the Raman spectrometer illustrated in FIG. 1A.

[0028] FIG. 2A is a schematic diagram of a patch system, with microprocessor comparison of signal and reference, that can be attached to a person to monitor for apoptosis post-operatively.

[0029] FIG. 2B is a schematic diagram of an alternative patch system utilizing a lock-in amplifier.

[0030] FIG. 3 illustrates use of a system for monitoring for cell apoptosis in a research environment for monitoring efficacy of a stimulant for producing cell apoptosis.

[0031] FIG. 4 is a schematic illustration of a network environment in which various embodiments can be used in connection with an efficacy analysis server.

[0032] FIG. 5A is a flow diagram illustrating a procedure for monitoring for apoptosis based on a Raman shift of about 569 cm^{-1} related to a change of state for cytochrome *c*.

[0033] FIG. 5B is a flow diagram illustrating a procedure for monitoring for apoptosis based on a Raman shift of about 675 cm^{-1} related to a change of physical state for cytochrome *b*

[0034] FIG. 6A is a flow diagram illustrating a procedure for detecting a stimulus efficacy for inducing apoptosis in a test cell.

[0035] FIG. 6B is a flow diagram illustrating a procedure similar to that of FIG. 6A except based on a scattering mode of cytochrome *b*.

[0036] FIG. 7 is a flow diagram illustrating a procedure for detecting a stimulus' efficacy for inducing apoptosis in a test cell that has been exposed to the stimulus, where the efficacy is a function of a control magnitude of a scattering signal at the Raman shift for a control cell that has not been exposed to the stimulus.

[0037] FIG. 8A is a graph showing the low-frequency resonance Raman spectra for intact reduced mitochondria from bovine heart (A) and rat liver (B), along with the spectrum of reduced cytochrome *c* in solution (C), with spectral intensities shown in arbitrary units (a.u.).

[0038] FIG. 8B is a graph showing the high-frequency resonance Raman spectra for intact reduced mitochondria from bovine heart (A) and rat liver (B), along with the spectrum of reduced cytochrome *c* in solution (C).

[0039] FIG. 9A is a graph showing time evolution of resonance Raman results obtained for bovine heart mitochondria loaded with Ca^{2+}.

[0040] FIG. 9B is a graph showing time evolution of resonance Raman results obtained for rat liver mitochondria loaded with Ca^{2+}.

[0041] FIG. 10 is a graph showing time dependence of Soret resonance Raman spectra in the high-frequency region of bovine heart (A) and rat liver (B) mitochondria loaded with Ca^{2+}.

[0042] FIG. 11A is a graph showing Soret resonance Raman spectra in the low-frequency region of the bovine heart (A) and rat liver (B) mitochondria supernatants.

[0043] FIG. 11B is a graph showing Soret resonance Raman spectra in the high-frequency region of the bovine heart (A) and rat liver (B) mitochondria supernatants.

[0044] FIG. 12A is a graph showing Soret resonance Raman spectra in the low-frequency regions for the bovine heart (A) and rat liver (B) mitochondrial pellets.

[0045] FIG. 12B is a graph showing Soret resonance Raman spectra in the high-frequency regions for the bovine heart (A) and rat liver (B) mitochondrial pellets.

[0046] FIG. 13 is a graph showing absorption spectra of cytochrome *c* released from swollen bovine heart (A) and rat liver (B) mitochondria as well as of ferrous cytochrome *c* in buffer solution (C).

[0047] FIG. 14 is a graph showing resonance Raman spectrum of cytochrome B5 in buffer solution obtained with 441.6 nm excitation.

DETAILED DESCRIPTION

[0048] A description of example embodiments of the invention follows.

[0049] There are distinct modes (i.e., vibrational frequencies) in cytochrome *c* that can be monitored using Soret band (blue wavelength) resonance Raman excitation, which change when cytochrome *c* is released into solution from the mitochondrial membrane. Monitoring these modes *in vivo* or *in vitro* will inform about the progress of cell death via apoptosis because cytochrome *c* release from the mitochondrial membrane initiates the apoptosis cascade. Apoptosis-sensitive modes may be monitored, *in vivo*, using fiber optics and hand-

held Raman devices. For example, that when open heart surgery is performed, the heart is taken offline via a heart bypass. When reperfusion takes place after surgery, there is a 2-3 day period when 20-30% of the patients (this is mostly children and babies with heart defects) apparently have serious problems and the heart does not recover. Currently the doctors don't have a good diagnosis tool, there is no indication that something is going wrong until it is too late, and fatalities occur. If apoptosis is initiated and starts to take place in the heart muscle following open heart surgery, an *in vivo* Raman probe could be a good indicator that gives advance notice of a problem and allows for more aggressive recovery procedures, prior to fatal dysfunction. The resonance Raman methodology can be used as a general way to diagnose the presence or absence of apoptotic cellular activity. This can be useful in a wide variety of medical procedures and diagnoses where doctors need to monitor tissue health. This can also be very useful in research applications where a real-time, label-free, method of monitoring apoptosis is desired.

[0050] The use of the documented difference in the vibrational properties of cytochrome *c* in the mitochondrial membrane versus the solution state presents a novel target for Raman spectroscopic imaging of cells that are undergoing apoptosis. This is because the loss of cytochrome *c* from the mitochondrial membrane is the primary cellular signal to begin apoptosis.

[0051] A specific novel feature of embodiment devices and methods is use of the mode near 570 cm^{-1} in the Raman spectrum that appears when cytochrome *c* folds tightly in solution and ruffles the heme group, turning on the selection rules that activate a variety of out-of-plane heme vibrational modes. In contrast to the solution state, these modes are absent when cytochrome *c* binds to the mitochondrial membrane.

[0052] A particular advantage is that Raman spectroscopy, where the presence of a new vibrational mode is a marker of cytochrome c in solution, is a label-free method of detecting apoptosis in live cells or tissue. Often a biochemical assay or introduction of a fluorescence label is used to detect apoptosis in cells using spatial imaging. In embodiments described herein, spatial imaging is not needed. Non-resonant Raman approaches are not specific to cytochrome *c*, and imaging can involve microscopes or other bulky equipment not suitable for a convenient hand-held or tissue patch device. Existing approaches can also be difficult to interpret, and statistical processing is usually necessary. Use of Soret excited resonance

Raman spectroscopy, targeting apoptotic changes in the cytochrome *c* Raman spectrum, is unique and provides a selective advantage over prior approaches.

[0053] In some embodiments, systems include a medical device used in an operating room or for post-operative diagnosis. Embodiments can also be used as a research tool where cell lines undergoing apoptosis are being monitored. Apoptosis is a key issue in developmental biology (differentiation of tissue types and morphology) as well as in cancer (cancer cells being resistive to apoptosis).

[0054] In some embodiments, systems can be configured to utilize (the now relatively common) hand-held Raman spectroscopy systems: Laser source, fiber optic delivery and collection, miniature monochomater, and detector. The use of stabilized diode lasers operating within the blue bandwidth (400-460nm) can be used as the excitation light source so the photon excitations are resonant with the strong electronic absorption band (Soret band) of heme proteins. Spectral libraries of healthy cells or tissue versus those undergoing apoptosis can be used to detect the changes taking place as apoptosis ensues. These changes are primarily taking place in the mitochondria of these cells and involve the loss of membrane bound cytochrome *c* into the solution state.

[0055] FIG. 1A illustrates a system 100 for detecting cell apoptosis. The system includes a laser source 102 configured to apply an incident excitation light wavelength 104 to a biological sample 106. The incident excitation wavelength 104 is in a resonance wavelength band for a heme group of cytochrome *c* in the biological sample 106. In particular, the heme group of cytochrome *c* absorbs light in the wavelength range of about 340-450 nm. As understood in the art of resonance Raman spectroscopy, applying excitation light having wavelengths that are in an absorption band of a target sample can dramatically increase the strength of inelastically scattered light from the target, thus facilitating detection and analysis of inelastically scattered light.

[0056] In FIG. 1A, the biological sample 106 is heart tissue of a person 108 having open heart surgery. The heart tissue includes a heart cell 110 having various mitochondria 112 in the cell. The mitochondria 112 typically include cytochrome *c* 116 in an unfolded state in a membrane 114 of the mitochondria. During a process of controlled death of the cell, cytochrome *c* leaves the mitochondrial membrane in the cell and enters the cytosol solution to become cytochrome *c* 116' folded in solution. In other embodiments, the cell can be a cancer cell, organ transplant cell or another cell that requires monitoring for apoptosis, for example.

Other example biological samples can include particular heart tissues, cancerous tissues, organ tissues to be transplanted, or any other tissues to be monitored for apoptosis. The system 100, and methods employing the system 100, could also be used to study tissue development in the lab. Tissue development to form higher level structures involves programmed cell death, for example to form fingers from the hand pad of a fetus undergoing development.

[0057] Furthermore, as illustrated hereinafter, in addition to *in vivo* samples, such as the heart tissue biological sample 106 of the person having open heart surgery, in other embodiments, biological samples can include *ex vivo* or *in vitro* specimens. Furthermore, in other embodiments, as illustrated in FIG. 2A, for example, embodiment devices can be used post-operatively. Thus, FIG. 1A illustrates only one application of many applications in which a system such as the system 100 can be used to monitor for apoptosis. Other example applications are illustrated in FIGS. 2A and 3, for example.

[0058] Some of the excitation light 104 incident on the biological sample 106 is scattered by the cytochrome *c* 116 in the unfolded state in the mitochondrial membrane 114, as well as by the cytochrome *c* 116' folded in the cytosol solution. In some embodiments, the excitation light 104 can be delivered to the biological sample 106 (and the inelastically scattered light 118 may be received at the Raman spectrometer 120) via a fiber light guide. However, in other embodiments, solely free space optics are used for light delivery and collection. Thus, applying the incident excitation wavelength or detecting the inelastic light scattering can include using the fiber light guide.

[0059] The inelastically scattered light 118 is detected by a Raman spectrometer 120, which measures the strength of the inelastically scattered light 118 as a function of Raman shift. In particular, the Raman spectrometer 120 can include a CCD detector (illustrated in FIG. 1B) that converts optical signals at each wavelength to electronic signals forming digitalized raw data 123. In other embodiments, an optical filter set to pass only the light within the 569 cm^{-1} Raman shifted band can be used as the primary (126) signal source, and another filter set to pass at the reference region Raman shift can be the secondary (128) signal source. The reference scattering region can include the 550 cm^{-1} background spectral region, for example. In other embodiments, a different background or other reference scattering region can be used, including a spectral region for a second Raman peak that varies inversely

with the 569 cm^{-1} Raman peak with respect to the change of cytochrome *c* from unfolded to folded state.

[0060] The signals can be detected synchronously with lock-in amplifiers by using modulated excitation light. If needed (not shown), output signals can be converted to digital format using a separate microcontroller, for example. Collection of the inelastically scattered light 118 and detection in the Raman spectrometer 120 are illustrated in further detail in FIG. 1B.

[0061] A processor 136 receives the electronic signals from the Raman spectrometer 120 and analyzes the signals by producing a graph 121. The graph 121 includes a Raman spectrum 122 with features reflecting the vibrational properties of the cytochrome *c* and any other light scatterers in the biological sample 106.

[0062] A peak 124 is particularly useful in monitoring for cell apoptosis in the biological sample because the peak is centered at an inelastic Raman shift of about 569 cm^{-1}, which first appears and then rises as cytochrome *c* increasingly falls out (is released) into the cytosol solution, as illustrated further hereinafter. For example, FIG. 8A shows measurements in which resonance Raman spectra of intact heart (A) and liver (B) mitochondria are compared with resonance Raman spectra of ferrous cytochrome *c* in a buffer solution (C). A peak at 569 cm^{-1} is not visible in the intact heart and liver mitochondria spectra, while the peak is visible in the buffer solution spectrum. Furthermore, FIG. 9B is a graph illustrating resonance Raman spectra obtained for rat liver at various times after cell apoptosis was induced by loading the mitochondria with Ca^{2+}. At the 5 minute time period, the spectrum does not show the peak at about 569 cm^{-1} (570 cm^{-1}). However, for increasingly longer exposure times, up to three hours, for example, a peak centered at 570 cm^{-1} becomes visible in the resonance Raman spectra in FIG. 9B. The processor 132 determines magnitudes of scattering signal at various Raman shifts in the spectrum 122, including a primary magnitude 126 of the peak 124 at 569 cm^{-1}.

[0063] As also indicated in FIGs. 1A, 9A and Fig. 9B, a peak at 675 cm^{-1} can be used as an alternative or supplement to the 569 cm^{-1} peak in other embodiments. As described further hereinafter, the peak at 675 cm^{-1} is present in scattering spectra for healthy biological samples, but this peak is diminished as cell apoptosis occurs. This behavior is thought to result from cytochrome *b* instead of cytochrome *c*, and the results of scattering magnitude with respect to healthy versus dying mitochondria are opposite those for cytochrome *c*. Thus,

a change of physical state of cytochrome *b* for dying mitochondria can lead to diminished Raman scattering signal at 675 cm^{-1}, indicating that apoptosis is occurring. Furthermore, in some embodiments, three channels can be monitored, including the example background reference 550 cm^{-1} and scattering modes at 569 cm^{-1} and 675 cm^{-1}, for example. Other peaks, such as the one at 688 cm^{-1}, can also be used as a reference signal to compare the relative intensity of the 675 cm^{-1} scattering mode.

[0064] Continuing to refer to FIG. 1A, the processor 136 also monitors the primary magnitude 126 over time, as illustrated in a graph 130. At a given threshold, the processor 136 outputs an indication that cell apoptosis has been indicated. This indication is delivered by an indicator 134 of cell apoptosis, which is also included in the system 100. The indication can be an alarm, a written or electronic report, or a visual display with an indication that cell apoptosis has occurred, for example. The indicator 134 can include hardware corresponding to the indication to be provided, such as an LED, buzzer, printer, or computer screen, for example.

[0065] In other embodiments, instead of simply measuring the primary magnitude 126 over time, the processor 136 can monitor the ratio of the primary magnitude 126 and a secondary magnitude 128 (an example of relative strength of the primary scattering signal with respect to the secondary scattering signal), for example. The secondary magnitude 128 can be a magnitude of the Raman spectrum 122 at 550 cm^{-1}, for example, which is a location in the Raman spectrum where the magnitude of the spectrum is relatively constant, regardless of whether the cytochrome *c* is in the unfolded or folded state. This can be referred to as a background reference measurement in a background reference region of the spectrum and can be useful for normalizing signal magnitudes obtained by the Raman spectrometer 120 and analyzed by the processor 136. A similar approach can be used to monitor the change in physical state of cytochrome *b*, and either a background or another reference signal provided by another Raman peak can be used as a secondary signal. Analysis of a ratio of magnitudes primary and secondary signals can be used to determine a stimulus' efficacy for producing apoptosis in a sample, as further described hereinafter.

[0066] In other embodiments, the secondary magnitude 128 can be at other reference locations (regions) in the Raman spectrum. The secondary magnitude preferably includes a magnitude measured for the same test cell of the biological sample for which the primary scattering signal is measured.

[0067] The primary magnitude 126 is preferably measured at the center of the peak 124 at 569 cm^{-1}. However, the primary magnitude can be measured at any spectral location that is about 569 cm^{-1} (i.e., anywhere in the range of the peak 124 where the magnitude of the spectrum increases for increasing cytochrome *c* 116' in solution relative to cytochrome *c* 116 in the unfolded state in the mitochondrial membrane 114). Furthermore, in some embodiments, the primary and secondary magnitudes are the strength of scattering signals integrated over portions of the spectrum 122. For example, the primary magnitude 126 can be the strength of the Raman scattering signal integrated over the peak 124. Moreover, in some embodiments, the Raman spectrum 122 is normalized such that the secondary magnitude 128 (background or other reference signal) is substantially zero. In FIG. 9B, for example, the peak 124 is determined to be centered at about 570 cm^{-1} due to measurement uncertainty.

[0068] While the system 100 includes a Raman spectrometer 120, in other embodiments, the system does not include a Raman spectrometer, but only optical detectors with narrowband filters configured to pass inelastically scattered light with particular wavelength bands of interest. For example, one embodiment system includes a narrowband filter that passes inelastically scattered light with wavelengths corresponding to Raman shifts of 569 ± 5 cm^{-1} in the Raman spectrum. Other embodiments include an additional detector and narrowband filter passing wavelengths of the inelastically scattered light corresponding to the 550 ± 5 cm^{-1} background reference or any other useful reference bandwith in the Raman spectrum. Furthermore, in yet other embodiments, three detection channels can be used, as described hereinabove, and such embodiments can include a third detector and corresponding narrowband filter passing desired wavelengths. Three-channel systems that incorporate a lock-in amplifier can include appropriate modifications to monitor the additional channel.

[0069] In some embodiments, the laser source 102 is part of the Raman spectrometer 120. In some embodiments, the laser source 102, Raman spectrometer 120, processor 132, and indicator 134 are part of a single device and structure. However, in various embodiments, these components can be in separate physical structures and can be connected via appropriate communications paths. Furthermore, the analyses leading to graphs 121 and 130 can be performed by separate processors in some embodiments. It will also be understood that, in the case of detectors and narrowband filters used in place of the Raman spectrometer 120, the monitoring of the primary magnitude 126 over time, as illustrated in graph 130, can be

performed directly from either digital or analog signals obtained from the detectors and any accompanying signal processors.

[0070] In some embodiments, a system for detecting cell apoptosis can include using modulated incident excitation light, such as the light obtained using a pulsed laser or optical chopper, for example. A lock-in amplifier may be used in conjunction with the Raman spectrometer 122 detect inelastic light scattering that is synchronous with the incident modulated light. The use of modulated light and synchronous detection has the potential advantage of increasing signal-to-noise ratios.

[0071] FIG. 1B is a more detailed illustration of the Raman spectrometer 120 in FIG. 1A. The inelastically scattered light 118 is redirected by a collection lens 105. A collimation lens 107 collimates the beam and directs it into the Raman spectrometer 120. A transmission diffraction grating 109 in the Raman spectrometer diffracts the light such that diffracted light 118' is spectrally dispersed onto a CCD detector 111. Raw, digitized data 123 are output from the CCD detector to be analyzed by the processor 136. In other embodiments, a scanning diffraction grating is used in conjunction with a photomultiplier tube and A/D converter instead of the CCD detector 111. Furthermore, in some embodiments, two or more diffraction gratings can be used as part of the spectrometer.

[0072] FIG. 2A illustrates a patch system 200a attached via a strap 253 to a person 108 recovering from open heart surgery. The patch system 200a, in contrast to the system 100 illustrated in FIG. 1A, is designed to provide all functions and apparatus necessary to determine whether apoptosis has been initiated within a compact structure that can be attached to the patient or near the patient for ease and convenience of use. The patch can take the form of a box, bag, module, wearable device, or other compact enclosure that that can be worn by, attached to, used nearby a patient or another biological sample. The patch system 200a also illustrates how a system can operate in ways that differ from how the system 100 in FIG. 1A operates.

[0073] The patch can be constructed as a rigid enclosure or as a flexible enclosure that can conform more comfortably to the human body for mounting or wearing. Example materials for a patch enclosure can include metals and plastics. In certain cases, biocompatible enclosure materials may be advantageous. An opening can be provided through the patch to permit excitation light to pass out of the patch toward the biological sample and to permit inelastically scattered light from the biological sample to be received

into the patch. In particular, the opening in the patch can accommodate an optical fiber or bundle of fibers, as illustrated in FIG. 2B.

[0074] While many different types of laser sources can be used to provide excitation light, in the patch system 200a, a diode laser 202 is mounted within the patch and used to provide the excitation light 104 so as to make the patch system 200a as compact as possible. In other embodiments, a laser source such as the diode laser 202 is mounted on the patch or otherwise associated with the patch. As with the system 100 in FIG. 1A, the excitation light 104 can be delivered to the biological sample 106 using an optical fiber, for example. In some embodiments, the patch can be configured to irradiate tissue in a biological sample covered by the patch, and the patch can also collect light via an array of optical fibers, for example, as further illustrated in FIG. 2B. The inelastically scattered light 118 can also be received via one or more optical fibers, for example, as further illustrated in FIG. 2B.

[0075] The patch system 200a is designed to monitor specific, narrow spectral regions of the Raman spectrum 122 illustrated in FIG. 1A. Thus, the Raman spectrometer 120 is not required. As an alternative, the patch system 200a is designed to use a beam splitter 238 and a mirror 240 to split the inelastically scattered light and to direct it appropriately toward respective narrowband optical filters 242a and 242b. In some embodiments, the inelastically scattered light 118 can also be directed within the patch system 200a using fiber-optic or integrated optical components, and the beam splitter 238 and mirror 240 can be fiber-based or otherwise solid-state optical components, as further illustrated in FIG. 2B, for example.

[0076] The narrowband filter 242a is configured to pass inelastically scattered light within the Raman shift range covered by the peak 124 illustrated in FIG. 1A, centered at around 569 cm^{-1} (or around 675 cm^{-1} for other embodiments, where cytochrome *b* may be applicable instead of, or in addition to, cytochrome *c*). The filter 242a is also configured to block light outside of the peak 124. This light that is passed is directed to a photodiode 244a, which is powered by a power supply line 246, and the electrical output is a primary magnitude in analog form. Thus, the beam splitter 238, optical filter 242a, and photodiode detector 244a mounted within the patch allow a magnitude of a primary scattering signal at a Raman shift that represents a vibrational scattering mode of cytochrome *c* in the folded state to be determined. Depending on the precise bandwidth of the optical filter 242a, this bandwidth may be representative of the optical power within a very narrow Raman shift range centered on the peak 124, such as a range from about 568 cm^{-1} to about 570 cm^{-1}.

However, in other cases, the filter 242a has a wider bandwidth, such that the magnitude of the signal output by the photodiode 244a represents the total power within the peak 124, plus some power outside the peak 244a. In all cases, limiting the bandwidth of the filter 242a to cover only the range of the peak 124 has the potential to increase the signal-to-noise ratio, increasing detection sensitivity.

[0077] A secondary magnitude of a secondary scattering signal at a different Raman shift representing a background (or other reference) range (region) of the Raman spectrum 122 is similarly obtained using the mirror 240, together with the narrowband filter 242b and secondary photodiode 244b. The narrowband filter 242b passes light that is centered at 550 cm^{-1}. As described hereinabove, in other embodiments, this spectral range can be centered at other locations in the Raman spectrum 122, particularly regions of the Raman spectrum that are relatively constant in magnitude with respect to cytochrome *c* being in the unfolded state in the mitochondrial membrane versus in the folded state in the cytosol solution. The reference region for the physical changes in cytochrome *b* may include either background ranges or other Raman bands.

[0078] Preferably, the region of the spectrum passed by the optical filter 242b does not overlap with the spectral region of the peak 124 centered at 569 cm^{-1} in order to maximize any contrast between the signal magnitudes output from the photodiodes 244a-b. In this way, the secondary magnitude output from photodiode 244b can serve as a normalizing signal for accurate interpretation of the magnitude of the signal provided by the photodiode 244a at 569 cm^{-1} in light of optical alignment detection efficiencies, artifacts of measurement drift, etc. Thus, while a normalizing background or other reference signal is not always required in all embodiments, it is preferable to have a normalizing background or other reference signal (e.g., 550 cm^{-1}) for each biological sample measured. Even in cases in which two signals representing the 569 cm^{-1} shift are measured for different samples (e.g., a test cell subjected to a stimulus that can cause apoptosis and a control cell that is not subjected to the stimulus), it is preferable to have both primary and secondary signals for each sample, where the primary signal is expected to increase (or decrease, for 675 cm^{-1}) as apoptosis begins to occur and the secondary (background or other reference) signal is expected to remain constant or move inversely relative to the primary signal during apoptosis. Trim potentiometers, for example, may be used in conjunction with the photodiodes 244a-b in order to compensate for any differences in conversion efficiency of the photodiodes or optical transmission of the

optical filters. In some embodiments, the system can be calibrated using cytochrome c in buffer solution where the ratio of signal to background is known.

[0079] The primary and secondary magnitudes output by the photodiodes 244b and 244a, respectively, are digitized using respective analog to digital (A/D) converters 248a-b. The digitized primary and secondary magnitudes output by the A/D converters are input to a microprocessor 249. In other embodiments, a lock-in amplifier can be used, as illustrated in FIG. 2B. Furthermore, in certain of these embodiments, the A/D conversion, microprocessor, and memory functions can be included within a lock-in amplifier.

[0080] Continuing to refer to FIG. 1A, the microprocessor 249 calculates a ratio of the primary magnitude to the secondary magnitude (the primary magnitude divided by the secondary magnitude). The ratio 252 is stored in memory 254 within the patch system. The memory 254 also stores a predetermined threshold ratio that indicates when apoptosis has begun to occur. The microprocessor 249 determines when the ratio 252 exceeds the predetermined threshold ratio and then sends an LED activation signal 258 to a LED indicator 234, which lights up on the outside of the patch system 200a to indicate that apoptosis has begun to occur. In other embodiments, the indicator can include a buzzer, audible signal, monitor screen, paper or electronic report, or other means to indicate that apoptosis has begun to occur.

[0081] The predetermined threshold ratio stored by the memory 254 can be determined by calibration of the patch system 200a. Calibration can be performed, for example, by purposely inducing apoptosis in a control biological sample under controlled conditions to determine the minimum ratio that reliably indicates that cytochrome *c* has begun to be released from (fall out of) the mitochondria and that apoptosis has begun to occur. These threshold ratios and other calibration data can be received via a communications path 256 carrying calibration/control data from an outside source, such as a control computer or server, for example. Preferably, the threshold ratio is determined using a particular patch system 200a since performance of optical components, electronics, etc. may have some statistical variation from system to system. Also, data 250 can be provided, optionally, to a server from the microprocessor 249. Use of such data by a server is described further hereinafter in connection with FIG. 4.

[0082] FIG. 2B illustrates an alternative patch system 200b that incorporates a lock-in amplifier 251. Use of the system 200b with lock-in amplification is preferable because

signal-to-noise ratios are potentially greater than in the case of the system 200a in FIG. 2A or even the Raman-spectrometer-based system 100 in FIG. 1A. In particular, where the primary and secondary signals are in close spectral proximity, as shown in the example of FIG. 1A, lock-in amplification can be helpful in, effectively, analyzing contrast between the two signals.

[0083] The patch system 200b includes a modulated diode laser 200' with built-in modulation to provide amplitude-modulated excitation light 104'. The system 200b also includes a fiber bundle 237 that is used as a detection interface between the patch and the person. The fiber bundle 237 includes pairs of detection fibers 239a and 239b that are mounted for detection of scattered light from spatially similar locations with respect to the biological sample. All of the fibers 239a are optically combined into a single one of the fibers 239a and filtered by a transmission grating with a spatial filter 243a, which is a notch filter tuned to the 569 cm^{-1} peak illustrated in FIG. 1A. A solid state waveguide combiner, for example, can be used to optically combine the signals. In similar fashion, all of the fibers 239b are optically combined into a single one of the fibers 239b and filtered by a transmission grating 243b, which is a notch filter tuned to the 550 cm^{-1} background reference region illustrated in FIG. 1A. Thus, the detection fibers 239a-b collect and spatially condense the scattered light to be filtered and converted to respective electrical signals via the detector photodiodes 245a-b.

[0084] In some particular embodiments, the patch includes an array of optical fibers with their active ends pointing perpendicular to a plane of the patch. The fibers collect scattered light and direct it perpendicular to the plane of the patch to inputs of respective optical combiners, filters, and detectors and electronics stacked outward perpendicularly with respect to the patch plane. The array of optical fibers in the patch can be coupled to human tissue through an index matching material, for example. An index matching material may have a viscous consistency similar to that of a transparent salve or ointment, for example. It is possible that an index matching material can also assist in adherence of fibers to tissue.

[0085] The two filtered optical signals in the fibers 239a and 239b are converted to analog electrical signals by the respective photodiodes 245a and 245b. The corresponding electrical signals are input at the A and B inputs, respectively, of the lock-in amplifier 251. The amplifier 251 also receives a modulation reference signal 247 from the modulated diode laser 202'. The amplifier 251 is configured to respond to the ratio (A/B) of the A input and

the B input. This ratio is a particularly meaningful signal and preferably used in this and other embodiments because it tends to eliminate the effects of instrumental drift, slight changes in optical alignment, changes in diode laser output, and other potential artifacts of system transients. In some embodiments, the detection fibers, optical combiners, transmission gratings, and photodiodes may be coupled using integrated optics, for example.

[0086] The lock-in amplifier 251 provides an output lock-in signal amplitude 255 that represents an integration of the laser modulation reference signal 247 with the ratio A/B of electrical signals described hereinabove. This output signal 255 is received by the microprocessor 249, which is programed to turn on the LED indicator 234 via the LED activation signal 258 when the reference signal 247 exceeds a specified threshold value. Similar to the device 200a in FIG. 2A, threshold values can be determined by appropriate device calibration and can be received into memory 254 via optional calibration/control data 256, for example. In certain embodiments, the microprocessor 249 and memory 254 can be combined into a lock-in amplifier.

[0087] FIG. 3 illustrates a bench test station 360 that can be used for detecting the efficacy of a stimulus for inducing apoptosis in a test cell that has been exposed to the stimulus. Such a system can be used for cancer research, drug discovery, or other laboratory or medical research applications in which the propensity of the stimulus to induce apoptosis must be determined. Various stimuli that can be studied can include drugs, chemicals, heat, cold, pressure, and any other variable whose propensity to induce apoptosis in cells is to be determined. Stimuli can also include particular treatment or surgical regimens, such as therapies for cancer or other illnesses or diseases. Stimuli can include treatments in the form of injections, pills, radiation therapy, light therapy, chemotherapy, or any other form that has a potential to affect cellular health.

[0088] In FIG. 3, a system 304 for monitoring for apoptosis includes internal components 362, which can include, for example, the elements in system 100 in FIG. 1A or the elements in the patch system 200a in FIG. 2A or similar elements. The system 300 can be a self-contained system, including a processor with analytical functions, such as the system 100 or 200a. However, in other embodiments, the system 300 includes only a spectroscopy subsystem such as the subsystem 101 in FIG. 1A, for example. In this case, signals produced from the light collection can be transmitted from the system 302 to an external processor for

analysis, as further illustrated in FIG. 4. In some embodiments, the system 300 can incorporate a hand-held Raman spectrometer.

[0089] An optical system 364 carries the excitation light from the system 300 to a biological sample. The optical fiber 364 is held over the sample using a fiber holder 365. The biological sample in FIG. 3 consists of cells 310 in a petri dish 366. A stimulus solution 368 in the petri dish is tested for its efficacy in producing apoptosis of the cells 310. Systems such as those illustrated in FIGS. 1A-3 can be used to carry out procedures such as those described hereinafter in connection with FIGS. 5A-5B, 6A-6B, and 7.

[0090] FIG. 4 illustrates a network environment in which various embodiments such as those illustrated in FIGS. 1A-3 can be used in connection with an efficacy analysis server 470. The efficacy analysis server 470 includes a processor 436 that can perform various functions, including the functions performed by the processor 136 in FIG. 1A and the microprocessor 249 in FIG. 2A. The server 470 communicates with the spectroscopy subsystem 101 in a hospital 472a, the patch subsystem 200a in a hospital 472b, and the benchtop system 300 in a research institution 472c via a wide area network 473 and various communications paths 474. The server 470 provides a remote analytical and data collection platform that can send and receive information to and from the various embodiments systems in different locations. Thus, information can be collected for research purposes, and analysis can be performed remotely to determine when apoptosis has occurred in a biological sample in any one of the facilities 472a-c. In other embodiments, the server 470 can be located in the same building, or even in the same room, as one or more embodiment systems. In such embodiments, communication between the server and the embodiment systems can be performed via a local area network, wireless interface such as Bluetooth, or other means of communication.

[0091] The hospital 472a includes only the spectroscopy subsystem 101 of the system 100 in FIG. 1A. These components include the laser source 102 and the Raman spectrometer 120 used to provide the excitation light to the biological sample and receive the inelastically scattered light from the sample, respectively. The subsystem 101 sends the raw, digitized spectroscopic data 123 over the network to the server 470. The processor 436 performs the functions of the processor 136 in FIG. 1A. It should be pointed out that, where a lock-in detector such as that illustrated in FIG. 2B is used at high modulation frequencies that eliminate 1/f noise and result in better signal-to-noise ratios for detection, it may not be

practical to send raw data values over a network. Instead, in these cases, it is preferable to perform lock-in functions locally at the detection location, and, if necessary, send the lock-in signal amplitude 255 over the network for further analytics, as illustrated in FIG. 2B.

[0092] Continuing to refer to FIG. 4, the processor 436 provides indicator results 475 back to the hospital 472 via the network 473. The indicator results 475 can include an indication that apoptosis of a cell in a biological sample in the hospital 472 has been initiated. The indicator results 475 can also include analyzed spectroscopic information, calibration instructions for the subsystem 101, reports, or other analytics produced from the raw data 123, such as the primary and secondary magnitudes 126 or 128, respectively.

[0093] The patch system 200a in the hospital 472b sends data 250 to the server 470 over the wide area network. The data 250 can include the ratio 252 calculated by the microprocessor 249 in FIG. 2A or any other results or data calculated by the microprocessor 249, such as the two digitized magnitudes 248a-b. The processor 436 sends the calibration/control data 256 over the network back to the patch system 200a to be stored in memory and used as necessary. The data 256 can include instructions for controlling the patch system 200a, calibration results or instructions, an indication that the patch system 200a requires service, or any other analytics that can be produced by the server 470 based on the raw data 250. Furthermore, in other embodiments, the patch system 200a sends additional data that can be used or stored by the server 470.

[0094] The system 300 and the research institution 472c sends data 476 over the network to the server 470. The system 300 also receives return data 477 from the server. The nature of the sent data 476 and return data 477 depend on the exact configuration of the system 300. For example, stimulus efficacy information obtained by the system 300 can be sent over the network and stored at the server 470 for analysis. The return data 477 can include various analytics, calibration/control data, or other information produced by the server 470.

[0095] One advantage of the interconnected network environment illustrated in FIG. 4 is that systems in various locations can be monitored, provided with calibration data, updated, or otherwise assisted. Furthermore, it may be desirable to have on-site systems at the locations 472a-c perform only raw data collection, while having the remote server 470 perform analytical functions or collect statistically data for multi-site studies, or to facilitate business models that include per-use fees for use of embodiment systems. Furthermore, it

will be understood that the network environment illustrated in FIG. 4 can include many more embodiment systems in other locations that are not illustrated in FIG. 4.

[0096] FIG. 5A is a flow diagram illustrating a procedure 500a for monitoring for apoptosis in the biological sample. At 580a, an incident excitation wavelength is applied to the biological sample. The incident excitation wavelength is in a resonance wavelength band for a heme group of cytochrome *c* in the biological sample. At 580b, inelastic light scattering within Raman shift at about 569 cm^{-1} is detected. The inelastic light scattering results from a vibrational scattering mode of cytochrome *c*, resulting in the Raman shift at about 569 cm^{-1}. At 580c, the biological sample is monitored for an increase in cytochrome *c* in a folded state in solution relative to cytochrome *c* in an unfolded state in a mitochondrial membrane of the cell to detect initiation of apoptosis of the cell in the biological sample. Monitoring the biological sample for the increase in cytochrome *c* in a folded state is based on the light scattering in the inelastic Raman shift at about 569 cm^{-1}.

[0097] FIG. 5B is a flow diagram illustrating a procedure 500b for monitoring for apoptosis in the biological sample. The procedure 500b is similar to the procedure 500a in FIG. 5A, except that a Raman shift of about 675 cm^{-1} is measured, which is related to a change of physical state of cytochrome *b*. At 581a, an incident excitation wavelength is applied to the biological sample. The incident excitation wavelength is in a resonance wavelength band for a heme group of cytochrome *b* in the biological sample. At 581b, inelastic light scattering within a Raman shift at about 675 cm^{-1} is detected. The inelastic light scattering results from a vibrational scattering mode of cytochrome *c*, resulting in the Raman shift at about 675 cm^{-1}. At 581c, the biological sample is monitored for a change of physical state of cytochrome *b* in solution relative to cytochrome *b* in a mitochondrial membrane of the cell to detect initiation of apoptosis of the cell in the biological sample.

[0098] In some embodiments of procedures 500a and 500b, the incident excitation wavelength is in a wavelength band of about 340-450 nm. Furthermore, in some embodiments, the procedures further include detecting inelastic light scattering with a Raman shift in a background or other reference scattering Raman shift region of the cytochrome *c* or cytochrome *b* with scattering strength that remains substantially constant with respect to either increasing cytochrome *c* in solution or the change of physical state of cytochrome *b*. An example of such background or other reference scattering is the 550 cm^{-1} background band illustrated in FIG. 1A. As used herein, the background or other reference scattering

remains "substantially constant with increasing cytochrome *c* in solution" or a "change of physical state of cytochrome *b*" where any statistical or measurement-related differences in scattering in the background or other reference scattering can be easily distinguished from changes in scattering strength at about 569 cm^{-1} or 675 cm^{-1} when cytochrome *c* begins to fall out of the mitochondrial membrane into solution or the cytochrome *b* undergoes changes in physical state. Where two inelastic light scattering bands are detected, including both the 569 cm^{-1} or 675 cm^{-1} band and a background or other reference scattering spectral region, respective detectors such as those illustrated in FIGs. 2A-2B can be used to monitor relative strengths of the Raman shifts at 569 cm^{-1} or 675 cm^{-1} and the background or other reference scattering region.

[0099] In some embodiments of the procedures 500a and 500b, applying the incident excitation wavelength or detecting the inelastic light scattering includes using a fiber light guide, such as the optical fiber 364 illustrated in FIG. 3. The biological sample can be an *in vivo* sample, such as the heart illustrated in FIG. 1A. However, in some embodiments, the biological sample is an *ex vivo* sample, such as an organ that has been extracted from a donor and is being preserved for an organ transplant operation or a research experiment, for example. In yet other embodiments of the procedures 500a and 500b, biological samples include *in vitro* samples, such as the cells 310 in the petri dish 366 in FIG. 3. In addition to monitoring for initiation of apoptosis of the cells in the biological sample, the detection of the increase in cytochrome *c* in the folded state in solution can be used as an indicator of poor mitochondrial health in the cell. Furthermore, other embodiment procedures can include calibration steps to calibrate a spectroscopic device such as the subsystem 101 or the patch system 200a. In some embodiments, calibration of a device can be performed by monitoring a biological sample while facilitating a process of cell apoptosis (i.e. intentionally killing cells in a sample while monitoring the signals produced to calibrate the system).

[00100] FIGs. 6A-6B further illustrate that in some embodiments, a background or other reference measurement is preferably used, as illustrated in FIGs. 1A and 2A-2B.

[00101] FIG. 6A is a flow diagram illustrating a procedure 600a for detecting a stimulus' efficacy for inducing apoptosis in a test cell that has been exposed to the stimulus. At 682a, a magnitude of the primary scattering signal at a first Raman shift that represents a vibrational scattering mode of cytochrome *c* in the folded state is determined. At 682b, the efficacy is determined as a function of the magnitude of the primary scattering signal compared to a

magnitude of a secondary scattering signal at a second Raman shift for a background reference measurement.

[00102] FIG. 6B is an alternative flow diagram illustrating a procedure 600b for detecting a stimulus' efficacy for inducing apoptosis in a test cell that has been exposed to the stimulus. At 683a, a magnitude of a primary scattering signal at a Raman shift that represents a vibrational scattering mode of cytochrome *b* is determined. At 683b, the efficacy of the stimulus is determined as a function of the magnitude of the primary scattering signal compared to a magnitude of a secondary scattering signal at a Raman shift for a background or other reference measurement.

[00103] Examples of magnitude of the primary scattering signal in procedures 600a and 600b can include the primary magnitude 126 of the peak 124 illustrated in FIG. 1A, the analog output of the photodiode 244a in FIG. 2A, and the digital output signal of the A/D converter 248a in FIG. 2A. Examples of magnitude of a secondary scattering signal in procedures 600a and 600b include the secondary magnitude 128 (background or other reference magnitude) illustrated in FIG. 1A, the analog output of the photodiode 244b in FIG. 2A, and the digital output of the A/D converter 248b in FIG. 2A.

[00104] A function of the magnitude of the primary scattering signal compared to a magnitude of the secondary scattering signal in procedures 600a and 600b can include, for example, the ratio 252 described in connection with FIG. 2A. However, in other embodiments, functions of the two magnitudes can vary. Determining the efficacy as a function of magnitude of the primary scattering signal compared with magnitude of the secondary scattering signal can be performed, for example, by determining how high the ratio 252 of the magnitudes increases for a given stimulus applied to the test cell, whether the ratio crosses a particular threshold value, or whether the ratio of magnitudes for on stimulus exceeds a ratio similarly measured for another stimulus.

[00105] Such procedures as illustrated in FIGs. 6A and 6B can be performed using the system 300 at the test station 360 illustrated in FIG. 3, for example, to measure apoptosis in cells in the petri dish 366. As described hereinabove, the system 300 can include components and functions similar to those of system 100 in FIG. 1A, system 200a in FIG. 2A, or variations thereof, for example.

[00106] FIG. 7 illustrates that in some embodiments, a control cell can also be used in addition to the test cell. In particular, FIG. 7 is a flow diagram illustrating a procedure 700

for detecting a stimulus' efficacy for inducing apoptosis in a test cell that has been exposed to the stimulus, where the efficacy is a function of a control magnitude of a scattering signal at the Raman shift for a control cell that has not been exposed to the stimulus.

[00107] At 790a, a test magnitude is determined. The test magnitude is of a scattering signal at a Raman shift that represents a vibrational scattering mode of cytochrome *c* in a folded state or cytochrome *b* in a physically altered state. A physically altered state of cytochrome *b* can include any change in physical characteristic, upon or after being exposed to the stimulus, that leads to a change in the test magnitude of the scattering signal. The exact physical alteration of state need not be known, but it should be recognized empirically that a change in scattering signal resulting from the physical state alteration is indicative of cell apoptosis occurring. The scattering signal is from a test cell that has been exposed to the stimulus. At 790b, the stimulus' efficacy is determined as a function of the test magnitude compared to a control magnitude of a scattering signal at the Raman shift from a control cell that has not been exposed to the stimulus. For example, if the control magnitude remains constant, while the test magnitude increases over a given threshold, the stimulus may be considered to have efficacy for producing apoptosis. Even where control cells are used, embodiment procedures preferably include use of respective reference signals and ratios, such as those provided by a background reference signal or other reference signal such as a second spectral peak. As described further hereinabove, the ratio is especially meaningful because it can mitigate effects of drifting optical alignment and other system transients. Furthermore, use of a modulated excitation light source and lock-in amplifier is preferred to increase signal-to-noise ratios, as illustrated in FIG. 2B, for example.

[00108] Control cells for procedure 700 may be located in a second petri dish similar to the dish 366 in FIG. 3. Measurements of the control cell and test cell can be completed in turn or simultaneously. In some embodiments, duplicate systems can be used for measurements of the control and test cells. Where the stimulus is a chemical, the chemical may be introduced into a petri dish in which the test cell is located, for example.

[00109] Embodiment procedures also can be modified from those illustrated in FIGs. 5A-5B, 6A-6B, and 7 to determine the efficacy of at least two stimuli for inducing apoptosis in cells that have each been exposed to a respective stimulus. For example, a test cell exposed to a first stimulus can be used and monitored by one system for behavior when exposed to the first stimulus. Subsequently, a different test cell of the same or different type as the first test

cell can be monitored by a second system when exposed, in a different sample or petri dish, for example, to a different respective stimulus. The stimulus that has greatest efficacy for inducing apoptosis can be selected based on a comparison of the respective efficacies of the stimuli. The efficacy can be a function of the primary scattering signal (e.g., at 569 cm^{-1} or 675 cm^{-1} Raman shift). Furthermore, a rate of change of the primary scattering signal can be used to determine efficacy of the stimulus. For example, where one stimulus induces apoptosis, leading to an increased primary scattering signal at 569 cm^{-1} relative to a second stimulus, the first stimulus can be considered to have greater efficacy for inducing apoptosis then the second stimulus.

[00110] In all cases where either a single or multiple stimuli are evaluated, a background reference signal or other reference signal is preferably measured and used as a reference for each biological sample and respective stimulus. Preferably, the lock-in amplification method described in conjunction with FIG. 2B is used for each stimulus sample, such that the relevant signal that is evaluated to determine stimulus efficacy is the lock-in amplified signal determined based on the ratio A/B of the primary and secondary (background or other reference) signals using the laser modulation signal as an integration reference for the lock-in amplifier. This method is preferable to greatly enhance signal-to-noise ratios and mitigate various types of measurement drift.

[00111] The test cell can additionally be monitored both before and after application of the stimulus. Two different scattering bands (e.g., 569 cm^{-1} and 675 cm^{-1}) and a background reference (e.g., 550 cm^{-1}) or a reference peak (e.g., 688 cm^{-1}) of the cytochrome *c* can be monitored simultaneously. As used herein, "simultaneously" denotes determining two signals within a short timeframe compared to a process of apoptosis or action of a stimulus. Thus, the signals can be measured one after the other, but with respect to application of the stimulus to the test cell, simultaneous indicates that two signals are measured during the same time frame with respect to any apoptosis occurring.

[00112] The primary and secondary signals can be continuously compared to determine efficacy of a stimulus.

INVESTIGATION OF CYTOCROME C CONFORMATIONAL STATUS

[00113] The conformational states of cytochrome *c* inside intact and Ca^{2+} -exposed mitochondria have been investigated using resonance Raman spectroscopy. Intact and

swelling bovine heart and rat liver mitochondria were examined with an excitation wavelength (413.1 nm) in resonance with the Soret transition of ferrous cytochrome *c*. The different *b*- to *c*-type cytochrome concentration ratio in mitochondria from two different tissues was used to help assign the Raman spectral components. Resonance Raman spectra were also recorded for mitochondria fractions (supernatants and pellets) obtained from swollen (Ca^{2+}- exposed) mitochondria after differential centrifugation. The results illustrate that cytochrome *c* has an altered vibrational spectrum in solution, in intact, and in swollen mitochondria. When cytochrome *c* is released from mitochondria, its Raman spectrum becomes identical to that of ferrous cytochrome *c* in solution. The spectra of mitochondrial pellets indicate that a small amount of structurally modified cytochrome *c* remains associated with the heavy membrane fraction. Indeed, spectroscopic shifts in the low-frequency fingerprint and the high-frequency marker-band regions suggest that membrane binding leads to a partial opening of the heme pocket and an alteration of the heme thioether bonds. The results support the conclusion that most cytochrome *c* molecules in mitochondria are membrane-bound and that the cytochrome *c* structure changes upon binding. Furthermore, changes in the resonance Raman active mode located at 675 cm^{-1} in the spectra of intact, swollen, and fractionated mitochondria indicate that b-type cytochromes may also undergo structural alterations during mitochondrial swelling and disruption.

[00114] Cytochrome *c* is essential for normal functioning of living cells, and ironically, it also plays a key signaling role during the process of cell death (apoptosis). In life and respiration, cytochrome *c* transfers electrons from cytochrome *c* reductase to cytochrome *c* oxidase. In apoptotic death, a key step in the initiation pathway is the translocation of cytochrome *c* from the mitochondrial membrane space into the cytosol. Numerous *in vitro* and *in vivo* studies have provided much information about the structure and the function of cytochrome *c*. Still, the precise physiological context of this protein in the living and dying cell remains poorly defined.

[00115] Cytochrome *c* is a six-coordinate low-spin heme iron species. The heme (iron protoporphyrin IX) has axial iron ligands at both the fifth and the sixth coordination positions: histidine (Hisl8) and methionine (MetSO). In addition, two cysteine residues (Cys14 and Cys17) attach the heme to the protein via thioether bonds. The heme has only limited access to the surface of the protein. It lies within a crevice lined with hydrophobic amino acids. Only the edge of one pyrrole ring and the adjacent Cysl7 thioether bond lie at

the surface. Cytochrome *c*, which is located primarily at the outer face of the inner mitochondrial membrane and its cristae, behaves as a peripheral protein (i.e., it can be removed from the membrane by relatively mild treatments such as changes in pH or ionic strength of the aqueous medium). Nevertheless, the details of cytochrome *c* redox activity and its mechanism of membrane binding are clearly complex.

[00116] Cytochrome *c* catalyzes electron transfer from cytochrome *c* reductase to cytochrome *c* oxidase (two intrinsic inner membrane proteins) as well as between adjacent cytochrome *c* molecules. It also participates in redox cycles with cytochrome *b5,* an outer membrane protein. Most interprotein electron-transfer reactions are preceded by the formation of reversible protein complexes that bring the interacting hemes into an almost coplanar alignment. Such an arrangement usually maximizes overlap between the electron wave functions of the interacting cytochromes.

[00117] While a membrane bound cytochrome *c* can perform electron transfer between cytochrome *c* reductase and cytochrome *c* oxidase, it must also be available in an unbound conformation to serve as an electron carrier from the inner membrane to the proteins bound in the outer membranes (e.g., with cytochrome *b5).* Investigations of the interactions between cytochrome *c* and various membrane systems suggest that mitochondrial cytochrome *c* is found in unbound as well as in several membrane-bound conformations, all of which are exchangeable See (Woitczak, L., and Sottocasa, G. L. (1972), *J. Membr. Biol. 7*, 313-324.) and (Matlib, M.A., and O'Brien, P.J. (1976), *Arch. Biochem. Biophys., 173*, 27-33).

[00118] A recent model of cytochrome *c* interaction with the membranes and membrane proteins suggests that this complex dynamic process is controlled by interplay of electrostatic and hydrophobic binding forces. Cytochrome *c* interacts with the phospholipids of the inner mitochondrial membrane. This interaction yields at least two different cytochrome *c* conformations. One is created through electrostatic interactions of the positively charged cytochrome *c* with negatively charged phosphate groups of phospholipids. The other is created when cytochrome *c* partially embeds itself into the membrane bilayer through hydrophobic interactions. The interaction of cytochrome *c* with the various redox protein partners potentially yields additional conformations.

[00119] The existence of multiple membrane-bound conformations of cytochrome *c* in mitochondria has been verified in studies of the two step release of cytochrome *c* from isolated rat liver mitochondria. First, the interaction between cytochrome *c* and its membrane-

anchoring associate cardiolipin must be disrupted to generate a pool of soluble cytochrome *c*. Thereafter, permeabilization of the outer membrane leads to the significant release of cytochrome *c*. It was demonstrated that solubilization of the two bound cytochrome *c* conformations requires different detachment stimuli. The electrostatically bound conformation is sensitive to ionic strength, surface-charge density, or pH, while hydrophobically bound conformations respond to a disturbance of the membrane structure or modification of the mitochondrial lipids, specifically, cardiolipin.

[00120] More support for the view of different binding environments for cytochrome *c* comes from investigations of mitochondrial cristae modifications during apoptosis. On the basis of the results of combined high-voltage electron microscopic tomography (HVEM) and biochemical measurements, Scorrano (Scorrano, L., *et al.*, (2002) *Development Cell*, 2, 55-67) concluded that a major part of cytochrome *c* in mitochondria is separated from the intermembrane space and is stored in cristae. These results are in good agreement with earlier functional estimates of Bernardi and Azzone (Bernardi, P. and Azzone, G.F. (1981) *J. Biol. Chem.*, 256(14), 7187-7192), which suggest that only 15-20% of cytochrome *c* is in the intermembrane space.

[00121] Interestingly, through recognition of different conformations of cytochrome *c* in apoptotic and necrotic T hybridoma cells with monoclonal antibodies, it was shown that the cytochrome *c* conformation, which activates apoptosis in these cells, is membrane bound. Specifically, immunofluorescence confocal microscopy revealed that conformationally altered cytochrome *c* in post-apoptotic T hybridoma cells remains associated with mitochondria. Moreover, the heavy membrane (mitochondria containing) fraction of post-apoptotic, but not of live cells, was functional in caspase activation. The supernatant of post-apoptotic mitochondria did not show a pro-apoptotic function. On the basis of these observations, it was suggested that the membrane-bound cytochrome *c* may be the relevant caspase coactivation factor in apoptosis. Involvement of membrane-bound cytochrome *c* in apoptosis appears contradictory considering that cytochrome *c* must interact with Apaf-1, dATP, and procaspase-9 in the cytosol to form an apoptosome. To resolve this issue, a more precise understanding of the possible mechanisms for cytochrome *c* translocation to cytosolic states is required.

[00122] Despite extensive work on the problem of cytochrome *c* binding, it remains unclear what kind of reorganizations the structure of native cytochrome *c* undergoes when the

protein associates with the membrane and whether the protein's structure pronouncedly differs depending on the type of binding (i.e., electrostatic or hydrophobic).

[00123] In the investigation described here, resonance Raman spectroscopy was used to examine the conformational states of cytochrome *c* in its native environment inside mitochondria. Vibrational spectroscopy has been recognized to be a sensitive tool, capable of revealing subtle changes in the molecular structure of proteins. The difficulty of applying this method to the complex mitochondrial system arises from the presence of several different heme proteins. Because the peaks of the electronic absorption bands of *c*- and b-type cytochromes are quite similar, it is difficult to resonantly enhance only one type of cytochrome in whole mitochondria. Nevertheless, this obstacle can be resolved by taking advantage of differences in the Raman marker bands of the purified *c*- and b-type cytochromes. In earlier work, Adar and Erecinska (Adar, F. and Erecinska, M. (1978) *Biochemistry*, 17, 5484-5488) obtained resonance Raman spectra of whole pigeon breast mitochondria using Q-band excitation (520.8, 530.9, and 568.2 nm). The results reported by these authors lack the low-frequency part of the spectra (below 600 cm^{-1}), which is important for identification of the axial heme ligands. Even so, they were able to conclude that the biochemical states of the hemes and/or their protein environments in the intact mitochondria are described from the native protein conformations in solution.

[00124] Here, Soret-band excitation (413.1 nm) has been used to obtain the resonance Raman spectra of mitochondria from two types of tissue (bovine heart and rat liver) under different physiological conditions. To obtain additional information on the putative structural changes of cytochrome *c* on/in mitochondrial membranes, data were collected from both intact mitochondria and mitochondria that were induced to swell and release cytochrome *c*. The observed differences are discussed in the context of interactions between the cytochromes and the mitochondrial membrane.

[00125] Materials And Methods

[00126] *Preparation of Rat Liver and Bovine Heart Mitochondria.* Note on abbreviations: EDTA, ethylenediaminietetmacetic acid; HEPES, *N-2-hydroxyethylpiperazine-N'-2-ethaneswulfonic* acid; UV, ultraviolet; BSA, bovine serum albumin; Pi, inorganic phosphate. Rat liver mitochondria were prepared by standard centrifugation procedures in MSH (210 mM mannitol, 70 mM sucrose, 5 mM HEPES, pH 7.5) buffer supplemented with 1 mM Na_2EDTA and 0.1% BSA. The last washing was performed in an EDTA-free medium, and

final mitochondria were suspended in MSH buffer without EDTA at 96 mg of protein/mL. Fresh mitochondria were used within 4 hours. Bovine heart mitochondria were prepared in MSE (220 mM mannitol, 70 mM sucrose, 0.2 mM EDTA, pH 7.2) buffer as described earlier and stored at 40 mg of protein/mL (-20 °C). The frozen mitochondria were rapidly thawed and used within 3 hours.

[00127] For experiments with mitochondria swelling and release of cytochrome *c,* the original medium was substituted with KCl buffer (150 mM KCl, 5 mM Tris-HCl, pH 7.4) and 200 nmol of Ca^{2+} per mg of protein was added in the presence of 5 mM Pi. A buffer with 150 mM KCl is a standard medium for detaching loosely bound cytochrome *c* from the inner membrane. About 3 hours after Ca^{2+} overload, the mitochondrial suspensions were centrifuged at 9800g for *5* minutes at 4 °C. It was demonstrated that this protocol washes electrostatically bound cytochrome *c* from the mitochondrial intennembrane space. Supernatants were additionally filtered through a 0.22 pm filter (Millex-GV) that allows soluble proteins but not mitochondrial fragments to pass through. The resulting supernatants and pellets were used for measurements of Raman and absorption spectra. All samples were measured in sealed square quartz cuvettes with a 3 mm optical path (NSG Precision Cells). The mitochondrial samples remained reduced at the protein concentration used.

[00128] *Cytochrome c.* Horse heart cytochrome *c* was purchased from Sigma-Aldrich and dissolved in 100 mM sodium phosphate buffer (pH 7.2). The sample was reduced with ascorbic acid.

[00129] *Raman spectroscopy.* All resonance Raman measurements were carried out at 413.1 nm (krypton ion laser, Coherent Innova 300) in a 90°-scattering geometry using a *Spex1870* spectrometer (2400 grating, 0.5 m focal length, slit width 100 μm). The output of the monochromator was coupled to a CCD detector cooled by liquid nitrogen (Princeton Instruments, Inc.). The experimental setup also includes focusing and collection optics and a holographic notch filter (Kaiser Optical system). A commercial software (Princeton Instruments, Inc.) provided elimination of the noise spikes in the spectra caused by cosmic rays. The average power at the sample was 12-15 mW for whole mitochondria and 5 mW for cytochrome *c* in solution. Signal-to-noise ratio was improved by several repetitive scans at a rate of 30 s exposure per scan (1 scan covers the spectral region of ~800 cm^{-1}). The spectra were calibrated using neat fenchone. The accuracy of absolute frequencies was ± 1 cm^{-1} and less than ±0.2 cm^{-1} for relative shifts of bands. Collection of a typical spectrum took 2 min.

Sample integrity was monitored by UV/visible spectroscopy before and after each resonance Raman experiment.

[00130] *UV and Visible Spectra.* UV and visible spectra were recorded with a Hitachi U-3410 spectrophotometer.

[00131] Results

[00132] The aim of this work was to explore vibrational spectra of cytochrome *c* in real time during the course of mitochondrial swelling and upon its release from disrupted membranes. Mitochondria from rat liver and bovine heart, which represent tissues having different functions and which also vary in structure and in cytochrome content, were prepared. Liver mitochondria contain relatively few cristae and, thus, have more matrix space and less inner membrane surface than heart muscle mitochondria. The heart mitochondria lack many of the enzymes found in liver mitochondria, their cristae are packed more densely, and less matrix space is available. Heart mitochondria are thought to possess more of the tightly membrane-bound cytochrome *c*. Likewise, the shape and volume of cristae can be expected to affect the diffusion of cytochrome *c* between intracristal and inter membrane compartments, as well as the fraction of cytochrome *c* bound to the inner membrane. Both liver and heart mitochondria were investigated because, in addition to the differences in cristae, they contain different relative concentrations of the various cytochromes, which helps in the assignment of the resonance Raman peaks.

[00133] The choice of 413.1 nm as an excitation wavelength provides conditions for a preferential resonant enhancement of low-frequency Raman modes of reduced cytochrome *c* because the absorption peak of its Soret band is at 415 nm. Nevertheless, one might also expect contributions to the Raman spectra (especially in the high-frequency region) from the reduced b-type cytochromes, which have Soret band maxima at 424, 430, and 432 nm, respectively, for b_{560}, b_{562} and b_{566} (inner membrane proteins) and at 423 nm for b_5 (outer membrane protein). Estimates of the cytochrome content of the mitochondria from these two tissues are as follows (1): bovine heart mitochondria 0.75 μmol of cytochrome $c + c_1$ per gram of protein and 0.5 μmol of cytochrome *b* per gram of protein; rat liver mitochondria 0.11 μmol of cytochrome $c + c_1$ per gram of protein and 0.1 μmol of cytochrome *b* per gram of protein. The concentration ratio of cytochrome $c + c_1$ to cytochrome *b* is 1.5:1 for bovine heart and 1:1 for rat liver. The preparations that were used had, respectively, in the bovine heart mitochondria 30 μM cytochrome $c + c_1$ and 20 μM cytochrome band in the rat liver

mitochondria 10.6 μM of cytochrome $c + c_1$ and 9.6 μM cytochrome b. It was anticipated that the different cytochrome ratios found in rat liver and bovine heart mitochondria could aid in the interpretation of the Raman spectra obtained at 413.1 nm. In the Discussion, it is assumed that the strongest enhancement occurs for ferrous cytochrome *c*. Possible interference from b-type cytochromes is taken into account.

[00134] *Raman Spectra of Intact Mitocondria.* FIGS. 8A-8B show the low- and high-frequency resonance Raman spectra, respectively, for intact reduced mitochondria from bovine heart and rat liver, along with the spectra of reduced cytochrome *c* in solution. FIGS. 8A-8B show Soret resonance Raman spectra of intact bovine heart (A) and rat liver (B) mitochondria obtained with 413.1 nm excitation in the low-frequency (FIG. 8A) and high-frequency (FIG. 8B) frequency regions along with the spectrum of ferrous cytochrome *c* in a buffer solution (C). In the spectrum of native cytochrome *c,* the peak position of ν_4 mode (cut off in the plot (C)) is at 1362 cm^{-1}. The fluorescence background signal is not conducive to obtaining well-resolved spectra from mitochondria. Spectra obtained by Adar and Erecinska (Adar, F. and Erecinska, M. (1978) *Biochemistry*, 17, 5484-5488) of pigeon breast mitochondria with visible excitation also exhibit fluorescence contamination. For a given set of experimental conditions (e.g., 15 mW laser power at the sample and averaging the final spectra over 4 scans of 30 s each), a better signal-to-noise ratio was observed for bovine heart mitochondria, which can be explained by the higher concentration of cytochromes in this sample and by the absence of fluorescent liver enzyme systems such as cytochrome P-450. Although this enzyme system is present in rat liver mitochondria in minor amounts as compared to other cytochromes (0.011 μmol/g of protein), fluorescence from the flavoproteins associated with the cytochrome P-450 system may not be negligible. The mode at about 490 cm^{-1} (FIG. 8A) arises from the quartz cuvette. Because of the poor optical quality of the samples (mitochondrial solutions are strongly opaque media), the excitation beam was aligned very close to the wall of the cuvette; thus, the low-frequency region of almost all spectra contain a trace of the quartz peak. To verify the reproducibility of the data, the measurements were repeated seven times for bovine heart and five times for rat liver mitochondria and obtained similar results.

[00135] *Raman Spectra of Swelling Mitochondria.* The introduction of Ca^{2+} ions leads to accumulation of calcium diacetate in the mitochondrial matrix and subsequent osmotic swelling proportional to the extent of Ca^{2+} uptake. In both mitochondrial preparations, the

original isolation media were substituted with high ionic strength KCl buffer, and Ca^{2+} was added in the presence of Pi to induce mitochondria swelling. The rationale of these experiments was to induce changes in the Raman spectra of the mitochondria, which undergo swelling and release cytochrome *c* into the extramitochondrial medium. It is expected that cytochrome *c* undergoes structural alterations during this process, specifically, a conversion from membrane-bound to soluble conformation, and we attempted to monitor these changes.

[00136] FIGS. 9A, 9B, and 10 show the results obtained for bovine heart and rat liver mitochondria loaded with Ca^{2+}. FIGS. 9A-9B show time evolution of Soret resonance Raman spectra in the low-frequency region of bovine heart (FIG. 9A) and rat liver (FIG. 9B) mitochondria loaded with Ca^{2+}. Spectra were obtained with 413.1 nm excitation at indicated time intervals. During the first 30-40 min after Ca^{2+} addition, significant changes were observed in the vibrational spectra in the region near 700 cm^{-1}. Specifically in the case of rat liver mitochondria, a decrease in the relative intensity of the 675 cm^{-1} band was observed (after about 1 h at 4 °C the band at 675 cm^{-1} became undetectable) and an emerging triplet structure between 680 and 700 cm^{-1}. In contrast, the triplet structure was not revealed in bovine heart mitochondria, but a sharp peak at 688 cm^{-1} appeared. At the same time, the spectra in the 300-500 cm^{-1} low-frequency region became more complex and evolved toward the 8-peak structure, which is a unique feature of soluble cytochrome *c*.

[00137] FIG. 10 shows time dependence of Soret resonance Raman spectra in the high-frequency region of bovine heart (A) and rat liver (B) mitochondria loaded with Ca^{2+}. Spectra were obtained with 413.1 nm excitation at indicated time intervals.

[00138] FIG. 10 illustrates that the data that were recorded in the high-frequency part of the Raman spectrum (above 900 cm^{-1}) suffer from a strong fluorescence background. Data scans were collected within ~20 min intervals for 4 h (the samples were kept at 4°C during signal acquisition), and after the runs both sample preparations were centrifuged. The resulting supernatants and pellets were probed independently, and the Raman spectra are shown in FIGS. 11 and 12, respectively. The spectrum, which was obtained for supernatants of swollen mitochondria (FIGS. 11A-11B) corresponds to that of native cytochrome *c,* while the pellets of swollen mitochondria (FIGS. 12A-12B) show a spectrum resembling that of intact mitochondria and differing from that of soluble cytochrome *c*.

[00139] FIGS. 11A-11B show Soret resonance Raman spectra in the low-frequency (FIG. 11A) and high-frequency (FIG. 11B) regions of bovine heart (A) and rat liver (B) mitochondria supernatants. Spectra were obtained with 413.1 nm excitation.

[00140] FIGS. 12A-12B show Soret resonance Raman spectra in the low-frequency (FIG. 12A) and high-frequency (FIG. 12B) regions of bovine heart (A) and rat liver (B) mitochondria pellets. Spectra were obtained with 413.1 nm excitation. In addition to the Raman spectra, the absorption spectra for supernatant of both rat liver and bovine heart mitochondria were also recorded, as seen in FIG. 13, where they can be compared with the absorption spectrum of reduced cytochrome *c* in buffer solution.

[00141] Discussion

[00142] The structural changes that cytochrome *c* undergoes upon binding to model membrane systems (polyanions, phospholipid vesicles, electrodes) have been investigated using a variety of biophysical techniques including resonance Raman spectroscopy, ^{1}H, ^{13}C, ^{31}P nuclear magnetic resonance, circular dichroism, and other spectroscopic and biochemical techniques. According to these studies, cytochrome *c* undergoes a wide range of conformational changes upon association with the model membranes. Generally, these studies demonstrated that binding of cytochrome *c* to model membrane systems creates a protein conformation with a destabilized tertiary structure but a nativelike helical secondary structure and a more open heme pocket as compared to the native protein. Electrostatic (or loose) binding of cytochrome *c* to the membrane does not yield significant changes in the protein conformation as shown by circular dichroism and resonance Raman measurements. The hydrophobic (or tight) interaction between the protein and the phospholipids, however, leads to protein penetration into the membrane bilayer and a partial loss of α-helical structure. Since protein-phospholipid interactions are considered to be a close simulation of the putative interaction of cytochrome *c* with the inner mitochondrial membrane, the structural information reported in the studies with artificial membranes is likely to hold also for cytochrome *c* inside mitochondria. However, support for this concept from a direct analysis of cytochrome *c* in the functioning mitochondrial membrane *in situ* is lacking.

[00143] The structures of heme proteins in general and of cytochrome *c* in particular have been scrupulously correlated with the frequencies of certain resonance Raman modes. The low-frequency region (~200-800 cm^{-1}) is informative for identification of the heme structural inhomogeneity and the axial ligation of the central iron atom. The high frequency or marker-

band region (1300-1700 cm^{-1}) reveals the oxidation *(v_4),* spin, and coordination state *(v_2, v_3)* of the heme iron atom. All of these frequencies correspond to skeletal vibrations of the porphyrin. The modes v_{10} and v_{19} also reflect the spin and coordination (5 or 6) state of the metal atom. These general rules apply to cytochrome *c,* but specific differences (relative to protoporphyrin IX) occur because of the existence of two covalent bonds -CH(SR)CH_3 at the 2 and 4 positions in the porphyrinring, which attach the heme to the polypeptide chain through two thioether bridges. The symbol R represents cysteine residues Cys14 and Cys17 in the 2 and 4 positions, respectively. The notation here is adopted from the paper by Hu and co-workers (Hu, S., *et al.*, (1993) *J. Am. Chem. Soc.* 115, 12446-12458), who provided complete assignment of cytochrome *c* resonance Raman spectra, using cytochrome *c* reconstituted with isotopically labeled hemes. At the 6 and 7 positions in the porphyrin ring, cytochrome *c* has two propionate groups, whose vibrations are also Raman active. Band frequencies are almost the same for ferric and ferrous cytochrome *c,* except for the high-frequency skeletal modes, which reflect the different extent of back-bonding. The relative intensities of the Raman modes for Fe^{2+} and Fe^{3+} cytochrome *c* species are also very similar, reflecting the minimal change in heme structure in the two oxidation states.

[00144] FIG. 13 shows absorption spectra of cytochrome *c* released from swollen bovine heart (A) and rat liver mitochondria (B) as well as of ferrous cytochrome *c* in buffer solution (C). Absorption spectrum of ferrous cytochrome *c* is downscaled by a factor of 9.

[00145] In general, the resonance Raman spectra of intact reduced mitochondria excited at 413.1 nm do not exactly replicate the spectrum of the native reduced cytochrome *c* (FIGS. 8A-8B). The mitochondria spectra display a complex pattern of bands, only some of which belong to reduced cytochrome *c*. A comparison of the spectra of the purified protein with the spectra of mitochondria reveals that mitochondria have new bands that are not spectral features of cytochrome *c* (e.g., 675, 1228, 1245, 1473, 1568, 1612, and 1622 cm^{-1}. Also, the 1362 cm^{-1} and the 1397 cm^{-1} bands of cytochrome *c* are downshifted in mitochondria spectra to 1360 cm^{-1} and 1393 cm^{-1}, respectively, and the 1300, 1314, 1547, and 1592 cm^{-1} modes of cytochrome *c* are not detected at all. On the other hand, the spectra obtained for bovine heart and for rat liver mitochondria show good agreement of their peak positions, although not all of the bands are equally enhanced in both spectra.

[00146] *Low-Frequency Region.* Low-frequency vibrational modes in the cytochrome *c* Raman spectrum create a unique eight-peak structure of closely spaced bands that clearly

distinguishes cytochrome *c* from other heme proteins. The number of vibrations is doubled as compared to other heme proteins and is considered an indicator of a closed heme crevice and a pronounced saddling of the heme group in cytochrome *c* resulting from the six-coordinate state and the existence of strong steric constraints on the heme. The characteristic four sets of doublet bands, clustered in the spectral region ~330-430 cm^{-1} , are assigned to the two porphyrin stretching modes v_{11}*(347* cm^{-1}) and v_{50}*(357* cm^{-1}), and the remaining three pairs are, respectively, C-C-C and C-C-S bending modes of the propionate (at the 6,7 positions) and thioether (at the 2,4 positions) groups (Hu, S., Morris, I. K., Singh, J. P., Smith, K. M., and Spiro, T. G. (1993) *J. Am. Chem. Soc 115*, 12446-12458).

[00147] In both of the intact mitochondria samples, the peak positions in the ~330-430 cm^{-1} region are well-correlated with cytochrome *c* modes (FIG. 8A), but the spectra lose their resolution, and a prominent octet is not clearly observed. The same effect was observed by Hildebrandt *et al.* (Hildebrandt, P. and Stockburger, M. (1989) *Biochemistry*, 28, 6710-6728 and Hildebrandt, P. (1990) *Biophys. Acta.*, 1040, 175-186) when cytochrome *c* was bound to an artificial membrane interface. This was explained as a consequence of a looser structure around the heme crevice in the membrane-bound protein, which could also be associated with weakening of the Fe-Met80 bond and/or a partial unfolding of the protein. When the protein is bound to the membrane, the tertiary structure and axial ligand interactions of the heme are relaxed, and as a consequence, the spectral pattern is in homogeneously broadened. The effect is stronger for bovine heart mitochondria, which may be related to the higher fraction of membrane-bound cytochrome *c* in this sample (because of dense packing of the inner membrane cristae). Careful inspection of the mitochondria and cytochrome *c* spectra reveals small (~2 cm^{-1}) frequency differences for some of the low-frequency bands. While in the case of well-resolved and/or isolated peaks these differences are real (e.g., the 1362 cm^{-1} peak), for the weak and poorly resolved bands we consider ±2 cm^{-1} to fall within the limits of detection error. Therefore, we do not report any significant frequency shifts for the bands in the low-frequency (~200-500 cm^{-1}) region.

[00148] FIGS. 9A, 9B, and 10 present the spectra of swelling mitochondria. Only the soluble form of cytochrome *c* is released when the mitochondria lose outer membrane integrity. A soluble (native) conformation of cytochrome *c* is characterized by the well-resolved octet of bands between 347 and 421 cm^{-1}. Examination of the dynamics of these bands reveals that the Raman spectra of swelling mitochondria in this region eventually attain

a well-resolved eight-peak structure that was not observed in the intact mitochondria. It is suggested that these changes reflect appearance of an increasing pool of free cytochrome *c* in the intermembrane space. The resonance Raman spectra of both bovine heart and rat liver mitochondria supernatants (the mitochondria preparations were fractioned after Ca^{2+} overload) in FIGS. 11A-11B show a one-to-one correspondence with the spectrum of reduced cytochrome *c*. These results obviously demonstrate that cytochrome *c* released from mitochondria converts to its solution phase conformation. The spectra of mitochondria pellets in the low-frequency region (FIG. 12A) are quite similar to that of intact mitochondria, which suggests that some fraction of cytochrome *c* remains bound to the inner membrane, even after the mitochondria have ruptured.

[00149] *Mid-Frequency Region Near 700 cm^{-1}*. The Raman spectra of mitochondria in the mid-frequency region around 700 cm^{-1} exhibit more dramatic changes with respect to the solution phase cytochrome *c* spectrum. The main difference is the appearance of a strong band at 675 cm^{-1} that is absent in cytochrome *c* spectra. This band is more strongly enhanced in the spectrum of rat liver mitochondria. A firm assignment of this band and during mitochondria swelling cannot be made based on the data of FIGS. 9A-9B. This band is absent in the spectrum of native cytochrome *c* and the mitochondria supernatants. It appears in the spectra of intact mitochondria and eventually vanishes as the mitochondria swell. Thus, it is conceivable that this band might signal interactions between the cytochrome *c* and the membrane lipids upon association. However, previous resonance Raman studies of the cytochrome *b-e* complex, cytochrome $b_{562\text{-}O}$, reduced mitochondria, and the present studies (FIG. 14) demonstrate that the band at 675 cm^{-1} is a common feature of b-type hemes.

[00150] FIG. 14 shows resonance Raman spectrum of cytochrome b_5 in buffer solution obtained with 441.6 nm excitation. It is noted that FIG. 14 shows illustrates that cytochrome b_5 has a strong band at 675 cm^{-1}. It is not clear from these data why the solution spectrum is present in healthy mitochondria and absent when the mitochondria die. It is possible that the b-type cytochromes are being degraded and the heme is falling out (released) simultaneously with cytochrome *c* release during the death cycle.

[00151] The use of 413.1 nm excitation could be expected to provide conditions for selective resonance enhancement of the vibrational modes of reduced cytochrome *c* since its Soret peak is at 415 nm. However, this argument is effective only for the low-frequency modes. As shown previously, the Raman excitation profiles of cytochrome *c* display strong

resonant enhancement up to one Raman quantum to the blue of the Soret band vibrational origin. The peak positions of the Soret bands of b-type cytochromes are red-shifted by 10-19 nm (500-1000 cm^{-1}) from 413.1nm; thus, excitation at this wavelength will minimize the interference from low frequency Raman scattering of *b*- type hemes. On the other hand, the potential for relatively strong Raman scattering of high frequency b-type heme modes, along with the fluorescent background present in the experimental data (e.g., FIG. 11B), does not allow quantitative determination of the contribution from b-type hemes in the high-frequency region of mitochondria. Therefore, on the basis of the available experimental data, it is difficult to unequivocally explain the dynamics of the 675 cm^{-1} mode during mitochondria swelling and protein release. However, it is likely that the observed spectral effects at 675 cm^{-1} can be attributed to b-type cytochromes and their transformations during mitochondrial swelling.

[00152] Based on the empirical observations alone, it is expected that a change of state of cytochrome *b* to a physically altered state leads to the scattering mode at 675 cm^{-1}. Thus, even without definite knowledge of the dynamics underlying the 675 cm^{-1} scattering mode, this mode is expected to be useful in place of the 569 cm^{-1} mode in any of the embodiment methods, devices, or systems described herein. The scattering mode at 675 cm^{-1} can thus indicate a change of state of cytochrome *b* to a physically altered state in solution relative to cytochrome *b* in a mitochondrial membrane of a cell, the change of physical state resulting in different scattering properties, to detect initiation of apoptosis. Appropriate adjustments to spectrometers, notch filters, detectors, etc. can be made to the apparatus and methods described hereinabove to monitor the 675 cm^{-1} scattering mode in place of the 569 cm^{-1} scattering mode, as will be understood by one of ordinary skill in the art. Furthermore, a three-channel system (monitoring 569 cm^{-1}, 675 cm^{-1}, and a background or other reference spectral location such as 550 cm^{-1} or 688 cm^{-1}) can be designed and be useful for redundant verification and indication of apoptosis occurring.

[00153] Another major discrepancy between the spectra of soluble cytochrome *c* and cytochrome *c* within the mitochondria is found in the region of the triplet centered near 692 cm^{-1}. In the Soret-excited spectrum of reduced cytochrome *c* there are three characteristic bands near 700 cm^{-1} a strong broad band at 692 cm^{-1} and two resolved shoulders at 682 and at 700 cm^{-1}. The shoulder at 700 cm^{-1} was identified as the ν_7 stretching mode, and the 682 and 692 cm^{-1} bands were assigned to C-S stretching of the two thioether groups.

[00154] The complex structure of the bands near 700 cm^{-1} is lost in intact mitochondria spectra, and only one peak can be resolved at 688 cm^{-1}. In both bovine heart and rat liver mitochondria spectra, the band at 688 cm^{-1} is weaker as compared to the band at 675 cm^{-1}; moreover, in the rat liver mitochondria spectrum the 688 cm^{-1} mode appears as a shoulder. However, the distribution of the amplitudes might be somewhat distorted because of a strong fluorescence background. The spectra of swelling bovine heart mitochondria do not show a noticeable shift of mode frequency, and the band at 688 cm^{-1} stays at the same position while the mitochondria undergo swelling and release of cytochrome *c*. The triplet structure of the bands centered at 692 cm^{-1} is not identifiable in the swelling bovine heart mitochondria. On the other hand, a clear triplet structure emerges in the spectrum of the bovine heart supernatant (FIG. 11A), and the correlation between the Raman frequencies of the supernatant with the modes of soluble reduced cytochrome *c* is excellent (682, 692, and 700 cm^{-1}). The pellets from bovine heart mitochondria (FIG. 12A) show a single 688 cm^{-1} band as found in intact and swelling mitochondria. The spectra of swelling rat liver mitochondria display a somewhat different behavior in the 700 cm^{-1} region. When mitochondria undergo swelling and the 675 cm^{-1} mode intensity decreases, the development of a triplet structure near 692 cm^{-1} is clearly seen.

[00155] The spectrum of rat liver mitochondria supernatant (FIG. 11A) (B) again is very similar to that of soluble reduced cytochrome *c*. The spectrum of rat liver pellets (FIG. 12A) (B) displays similarity with the intact mitochondria spectrum in the low-frequency region, but the structure of the bands near 700 cm^{-1} is slightly changed: the band at 688 cm^{-1} converts from a shoulder (FIG. 8A) to a peak, and a weak shoulder is recognizable at 682 cm^{-1}.

[00156] Taken together, these data suggest that in the intact mitochondria a major part of cytochrome *c* molecules are in the membrane-bound conformation, and binding to the membrane causes alterations in the structure of the triplet bands near 692 cm^{-1}. The room temperature Soret-excited resonance Raman spectrum of native (soluble) ferrous cytochrome *c* has two clearly resolved thioether (C_a-S) stretching bands at 692 and at 682 cm^{-1}. At low temperature, the complex triplet envelope resolves into three distinct bands. Detailed analysis of the cytochrome *c* enhancement pattern demonstrated that the cytochrome *c* π-π^* excited-state undergoes a large expansion along coordinates that involve substantial (C_a-S) stretching. Because the (C_a-S) bonds attach the heme to the protein, binding to the membrane might perturb these linkages and affect the Raman intensity. Detachment of the protein from the

membrane would restore the original solution structure of the protein. Therefore, one can observe the emerging triplet structure of the bands near 680-700 cm^{-1} during mitochondria swelling and the clear appearance of all three bands in the supernatant solution samples. The fact that the appearance of the triplet structure during swelling is noticeable only for rat liver mitochondria may be explained by the differences between the membrane structure in bovine heart and rat liver mitochondria. The membrane of bovine heart mitochondria contains many more cristae that are likely to retain cytochrome *c* during the swelling process so that less material is converted into the free solution phase.

[00157] Additional indirect evidence that cytochrome *c* is more easily released from swelling rat liver mitochondria comes from the absorption spectra of the supernatants (FIG. 13). Although it is speculative to use the absorption spectra obtained under these conditions to provide quantative information about the concentration of the released cytochrome *c,* they do show qualitatively that the amount of released cytochrome *c* is higher for rat liver mitochondria. We used the same quantities of the two·mitochondria preparations (about 3 mL) for pelleting, and the absorption spectra were measured in matched cuvettes (optical path is 3 mm). FIG. 13 also presents the absorption spectrum of reduced cytochrome *c* in buffer solution. Comparison of the spectra in FIG. 13 shows a good agreement between the absorption peak positions of the cytochrome *c* released from mitochondria and native ferrous cytochrome *c.*

[00158] *High-Frequency Region.* The inability to clearly resolve all of the high-frequency Raman modes of bovine heart and rat liver mitochondria limits the analysis. The high-frequency region (1200-1700 cm^{-1}) includes the oxidation, core-size, and spin marker bands v_4, v_3, v_2 and v_{10}. For these modes, correlations between frequencies and electronic configuration, core size, and ligation state of the heme iron are well-established. For reduced cytochrome *c,* these marker bands are located at 1362, 1492, 1592, and 1622 cm^{-1}, which are the positions expected for a 6-coordinate low-spin heme.

[00159] One of the spin state marker bands, v_3, in mitochondria is found at 1493 cm^{-1}, which correlates well with native reduced cytochrome *c* and corresponds to the low-spin state (FIG. 8B). The other spin-state marker is found at 1473 cm^{-1} and conceivably reflects the emergence of a pool of high-spin cytochromes. However, the α-type heme of cytochrome *c* oxidase also has a weak v_{28} mode at 1472 cm^{-1}. The Soret band peak position of cytochrome *c* oxidase is found at 445 nm, and the resonance Raman spectra of intact reduced

mitochondria, obtained by Adar and Erecinska (Adar, F. and Erecinska, M., (1979) *Biochemistry*, 18, 1825-1829) using the 441.6 nm HeCd laser line, show a weak band at 1472 cm^{-1}. A band at 1472 cm^{-1} was also resolved in the spectrum of soluble cytochrome *c* oxidase, excited at 413.1 nm. This band was slightly smaller with respect to the v_3 mode of ferric cytochrome *c,* obtained under similar experimental conditions (Figure 5A,B in (Dopner, S., et. al., (1999) *Europ. J. Biochem.*, 261, 379-391)). In our preparations, the cytochrome *c* oxidase concentration is calculated to be approximately 40 *pM* (the values for cytochrome content of isolated mitochondria are found in Table 4.7 of (Tyler, D. (1992) *The mitochondrion in health and disease*, VCH Publishers, New York)). The cytochrome *c* concentration is found to be 30 μM for bovine heart and 10.6 μM for rat liver mitochondria, respectively. It is therefore possible, or even likely, that the weak 1472 cm^{-1} mode of cytochrome *c* oxidase is enhanced sufficiently at 413.1 nm to become visible relative to the 1493 cm^{-1} mode of ferrous cytochrome *c* as observed in the mitochondria spectra of FIG. 8B.

[00160] The oxidation state marker band v_4 is downshifted in mitochondria by 2 cm^{-1}. In reduced cytochrome *c,* this band has a small shoulder at 1397 cm^{-1} (FIG. 8B) that is also downshifted in mitochondria to 1393 cm^{-1}. The positions of v_4 and the shoulder in supernatant preparations are found at 1362 and 1398 cm^{-1}, which are the same as in native cytochrome *c.* In the pellet preparations of bovine heart and rat liver mitochondria, v_4 is found at 1362 cm^{-1}. An upshift of v_4 or the appearance of a shoulder at 1372 cm^{-1}, if observed, would indicate a change from the fully reduced state to one with an oxidized population of cytochromes (the oxidized cytochrome *c* has v_4 at 1372 cm^{-1}). Such changes are not observed; thus, the cytochrome *c* remains in the fully reduced state. The downshift of v_4 by 2 cm^{-1} is assigned to perturbations associated with the protein membrane interaction. The behavior of this band during mitochondria swelling and cytochrome *c* release gives support to the hypothesis that the changes are due to protein intercalation in the inner membrane. It is noted that v_4 in rat liver and bovine heart pellets (FIG. 12B) remains at 1360 cm^{-1} as found for intact mitochondria, while in both supernatants this mode is observed at 1362 cm^{-1} similar to native cytochrome *c.* Therefore, some fraction of cytochrome *c* remains in the bound conformation within the membrane remnants formed after mitochondria swelling and centrifugation. This observation is in agreement with the estimation of Cortese *et al.* (Cortese, J.D., *et al.* (1998) *Biochemistry*, 37, 6402-6409), who reported that approximately 11% of cytochrome *c* remains bound to inner mitochondria membrane at ionic strength ~150 mM.

[00161] The ν_2 band at 1592 cm^{-1} is not clearly resolved in mitochondria spectra, but a shoulder at 1623 cm^{-1} is detected, which can be assigned to the ν_{10} mode. These spectral features are consistent with the heme in mitochondria being in a ferrous low-spin state.

[00162] Unambiguous assignments of the bands observed in the mitochondria spectra at 1245, 1523, 1568, and 1612 cm^{-1} are intricate in the absence of additional information. These bands are not spectral features of native cytochrome *c*. They also were not detected in the spectra of purified cytochrome b_5 and cytochrome b_{566} at Q-band excitation (except 1612 cm^{-1} which is very weak in the cytochrome b_{566} spectrum with 568.7 nm excitation). However, some of these bands (a weak shoulder at 1568 cm^{-1} and a well- resolved band at 1610 cm^{-1}) were observed in mitochondria spectra with 441.6 nm excitation, which provides preferable enhancement for cytochrome *c* oxidase and indicates that this species also contributes weakly to the Raman spectra obtained using 413 nm excitation.

[00163] In summary, these experiments reveal that the changes in protein conformation that were previously reported when cytochrome *c* binds to artificial and natural membrane systems are qualitatively similar to the transformations that occur when cytochrome *c* is attached to the inner mitochondria membrane. This gives support to the idea that protein-phospholipid model systems provide an important and reliable test bed for studies of protein-membrane interactions. Cytochrome *c* molecules in mitochondria are found primarily in the membrane-bound state, and binding evidently causes a partially opening of the heme pocket and alteration of the heme-Cys 14 and heme-Cys 17 thioether bonds. As mitochondria swell, a significant pool of free (solution phase) cytochrome *c* is created through detachment of the protein from the membrane. This pool is released once the outer membrane is permeabilized. Also, there is a portion of the cytochrome *c* that remains bound to the inner membrane even after the mitochondria are overloaded with Ca^{2+} and swell to the breaking point. This signifies the existence of a tightly bound protein fraction. Finally, the experimental data (i.e., the dynamics of the 675 cm^{-1} mode) suggest that not only cytochrome *c,* but also the cytochrome *b* proteins, undergo transformation as the outer membrane is altered during mitochondrial swelling and rupture.

[00164] The description hereinabove addresses key spectroscopic aspects of cytochrome *c* binding to mitochondrial membranes. Cytochrome *c* undergoes a conformational change early in apoptosis and necrosis, which is not due to a covalent modification but is consistent with a membrane association induced transformation. The release of cytochrome *c* from its

membrane bound state in the mitochondria is a fundamental signaling mechanism for cell death. The ability to understand and control the process of cytochrome *c* binding and release from the mitochondrial membrane would likely have significant ramifications in our ability to treat human cancer cells, many, if not all of which, display a strong resistance to apoptosis.

[00165] In addition to other publications cited herein, the following paper is hereby incorporated by reference herein in its entirety: Sun., Y., Benabbas, A., Zeng, W., Kleingardner, J.G., Bren, K.L., and Champion, P.M. (2014) "Investigations of Heme Distortion, Low-Frequency Vibrational Excitation, and Election Transfer in Cychrome c," PNAS, 111(18): 6670-6575.

[00166] The teachings of all patents, published applications and references cited herein are incorporated by reference in their entirety.

[00167] While this invention has been particularly shown and described with references to example embodiments thereof, it will be understood by those skilled in the art that various changes in form and details may be made therein without departing from the scope of the invention encompassed by the appended claims.

CLAIMS

What is claimed is:

1. A system for monitoring for cell apoptosis, the system comprising:

a patch configured to be applied to a person;

a laser source in the patch, the laser source configured to apply an incident excitation wavelength to a biological sample, the biological sample being part of the person;

a detector in the patch, the detector configured to detect light scattering, caused by the incident excitation wavelength, from the biological sample; and

a processor configured to monitor a state of the biological sample based on the light scattering.

2. A method of monitoring for apoptosis in a biological sample, the method comprising:

applying an incident excitation wavelength to the biological sample, the incident excitation wavelength being in a resonance wavelength band for a heme group of cytochrome *c*;

detecting inelastic light scattering with a Raman shift at about 569 cm^{-1}, the inelastic light scattering resulting from a vibrational scattering mode of cytochrome *c*, resulting in the Raman shift at about 569 cm^{-1};

monitoring the biological sample, based on the light scattering with the inelastic Raman shift at about 569 cm^{-1}, for an increase in cytochrome *c* in a folded state in solution relative to cytochrome *c* in an unfolded state in a mitochondrial membrane of a cell to detect initiation of apoptosis of the cell in the biological sample.

3. A system for detecting cell apoptosis, the system comprising:

a laser source configured to apply an incident excitation wavelength to a biological sample, the incident excitation wavelength in a resonance wavelength band for a heme group of cytochrome *c*;

a detector configured to detect inelastic light scattering with a Raman shift at about 569 cm^{-1}, the inelastic light scattering resulting from a vibrational scattering mode of the cytochrome *c*; and

a processor configured to monitor the biological sample, based on the light scattering in the inelastic Raman shift at about 569 cm^{-1}, for an increase in cytochrome c in a folded state in solution relative to cytochrome *c* in an unfolded state in a mitochondrial membrane of a cell to detect initiation of apoptosis of the cell in the biological sample.

4. A method of detecting a stimulus' efficacy for inducing apoptosis in a test cell that has been exposed to the stimulus, the method comprising:

determining a magnitude of a primary scattering signal at a first Raman shift that represents a vibrational scattering mode of cytochrome *c* in a folded state; and

determining the efficacy as a function of the magnitude of the primary scattering signal compared to a magnitude of a secondary scattering signal at a second Raman shift for a reference measurement.

5. A method of monitoring for apoptosis in a biological sample, the method comprising:

applying an incident excitation wavelength to the biological sample, the incident excitation wavelength being in a resonance wavelength band for a heme group of cytochrome *b*;

detecting inelastic light scattering with a Raman shift at about 675 cm^{-1}, the inelastic light scattering resulting from a vibrational scattering mode of cytochrome *b*, resulting in the Raman shift at about 675 cm^{-1};

monitoring the biological sample, based on the light scattering with the inelastic Raman shift at about 675 cm^{-1}, for a change of physical state of cytochrome *b* in solution relative to cytochrome *b* in a mitochondrial membrane of a cell to detect initiation of apoptosis of the cell in the biological sample.

6. A system for detecting cell apoptosis, the system comprising:

a laser source configured to apply an incident excitation wavelength to a biological sample, the incident excitation wavelength in a resonance wavelength band for a heme group of cytochrome *b*;

a detector configured to detect inelastic light scattering with a Raman shift at about 675 cm^{-1}, the inelastic light scattering resulting from a vibrational scattering mode of the cytochrome *b*; and

a processor configured to monitor the biological sample, based on the light scattering in the inelastic Raman shift at about 675 cm^{-1}, for a change of physical state of cytochrome *b* in solution relative to cytochrome *b* in a mitochondrial membrane of a cell to detect initiation of apoptosis of the cell in the biological sample.

7. A method of detecting a stimulus' efficacy for inducing apoptosis in a test cell that has been exposed to the stimulus, the method comprising:

determining a magnitude of a primary scattering signal at a first Raman shift that represents a vibrational scattering mode of cytochrome *b*; and

determining the efficacy as a function of the magnitude of the primary scattering signal compared to a magnitude of a secondary scattering signal at a second Raman shift for a reference measurement.

8. A method of detecting a stimulus' efficacy for inducing apoptosis in a test cell that has been exposed to the stimulus, the method comprising:

determining a test magnitude of a scattering signal at a Raman shift that represents a vibrational scattering mode of cytochrome *c* in a folded state, or cytochrome *b* in a physically altered state, from a test cell that has been exposed to a stimulus; and

determining the stimulus' efficacy as a function of the test magnitude compared to a control magnitude of a scattering signal at the Raman shift that represents the vibrational scattering mode of cytochrome *c* in the folded state from a control cell that has not been exposed to the stimulus.

9. The system or method of any of Claims 1-8, wherein the incident excitation wavelength is in a resonance wavelength band for a heme group of cytochrome *c* or cytochrome *b*.

10. The system or method of any of Claims 1-9, wherein the detector is further configured to detect inelastic light scattering with a Raman shift at about 569 cm^{-1}, the inelastic light scattering resulting from a vibrational scattering mode of cytochrome *c*, resulting in the Raman shift at about 569 cm^{-1}.

11. The system or method of any of Claims 1-10, wherein the detector is further configured to detect inelastic light scattering with a Raman shift at about 675 cm^{-1}, the inelastic light scattering resulting from a vibrational scattering mode of cytochrome *b*, resulting in the Raman shift at about 675 cm^{-1}.

12. The system or method of any of Claims 1-11, wherein the processor is further configured to monitor the state of biological sample, based on light scattering at an inelastic Raman shift of about 569 cm^{-1}, for an increase in cytochrome *c* in a folded state in solution relative to cytochrome *c* in an unfolded state in a mitochondrial membrane of a cell to detect initiation of apoptosis of the cell in the biological sample.

13. The system or method of any of Claims 1-12, wherein the processor is further configured to monitor the state of biological sample, based on light scattering at an inelastic Raman shift of about 675 cm^{-1}, for a change of state of cytochrome *b* in solution relative to cytochrome *b* in a mitochondrial membrane of a cell to detect initiation of apoptosis of the cell in the biological sample.

14. The system or method of any of Claims 1-13, wherein applying the incident excitation wavelength in a resonance wavelength band includes using a wavelength band of about 340-450 nm.

15. The system or method of any of Claims 1-14, further including detecting inelastic light scattering with a Raman shift in a reference scattering region of the cytochrome *c*, a scattering strength of the reference scattering remaining substantially constant with increasing cytochrome *c* in solution.

16. The system or method of any of Claims 1-15, wherein detecting inelastic light scattering with a Raman shift at about 569 cm^{-1} and detecting inelastic light scattering with the Raman shift in the reference scattering region include using respective detectors to monitor relative strengths of the Raman shift at about 569 cm^{-1} and the Raman shift in the reference scattering region.

17. The system or method of any of Claims 1-16, wherein applying the incident excitation wavelength or detecting inelastic light scattering includes using a fiber light guide.

18. The system or method of any of Claims 1-17, wherein applying the incident excitation wavelength includes using modulated light, and wherein detecting the inelastic light scattering includes detecting the inelastic light scattering synchronously with the incident modulated light.

19. The system or method of any of Claims 1-18, further including calibrating a spectroscopic device used to monitor the biological sample by facilitating a process of cell apoptosis.

20. The system or method of any of Claims 1-19, wherein the cell is a heart cell, cancer cell, or organ transplant cell.

21. The system or method of any of Claims 1-20, wherein the biological sample is an *in vivo* sample, *ex vivo* sample, or *in vitro* sample.

22. The system or method of any of Claims 1-21, further comprising using the increase in cytochrome c in the folded state in solution as an indicator of poor mitochondrial health in the cell.

23. The system or method of any of Claims 1-22, wherein the laser source and the detector are mounted within a patch configured to be applied to a person.

24. The system or method of any of Claims 1-23, wherein the processor is located remotely from the laser source and detector, and wherein the processor is further configured to monitor using signals received from the detector via a signal path.

25. The system or method of any of Claims 1-24, further comprising an optical fiber configured to deliver the light from the laser source to the biological sample or to deliver scattering light from the biological sample to the detector.

26. The system or method of any of Claims 1-25, wherein the magnitudes of the primary and secondary scattering signals are determined simultaneously.

27. The system or method of any of Claims 1-26, further comprising:

receiving the magnitude of the primary scattering signal in the form of data, transmitted across a network communications path, at a server; and

transmitting, from the server, a representation of the efficacy via the network communications path.

28. The system or method of any of Claims 1-27, further comprising:

receiving the magnitude of the primary scattering signal in the form of data at a processor; and

outputting, by the processor, a representation of the efficacy.

29. The system or method of any of Claims 1-28, further comprising:

determining the efficacy of at least two stimuli for inducing apoptosis in cells that have each been exposed to a respective stimulus; and

selecting a stimulus based on a comparison of the efficacy of the stimuli.

30. The system or method of any of Claims 1-29, wherein determining the efficacy as a function of the magnitude of the primary scattering signal compared to a magnitude of a secondary scattering signal includes analyzing a ratio of the magnitudes of the primary and secondary scattering signals.

31. The system or method of any of Claims 1-30, wherein the magnitude of the primary or secondary scattering signal is an amplitude signal of the primary or secondary scattering signal, respectively.

32. The system or method of any of Claims 1-31, further including detecting inelastic light scattering with a Raman shift in a reference scattering region of the cytochrome *b*, a scattering strength of the reference scattering remaining substantially constant with respect to the change of state of cytochrome *b* in solution relative to cytochrome *b* in the mitochondria.

33. The system or method of any of Claims 1-32, wherein detecting inelastic light scattering with a Raman shift at about 675 cm^{-1} and detecting inelastic light scattering with the Raman shift in the reference scattering region include using respective detectors to monitor relative strengths of the Raman shift at about 675 cm^{-1} and the Raman shift in the reference scattering region.

34. The system or method of any of Claims 1-33, wherein the test magnitude and control magnitude are determined simultaneously.

35. The system or method of any of Claims 1-34, wherein determining the stimulus' efficacy includes analyzing a ratio of the magnitudes of the scattering signals from the test and control cells.

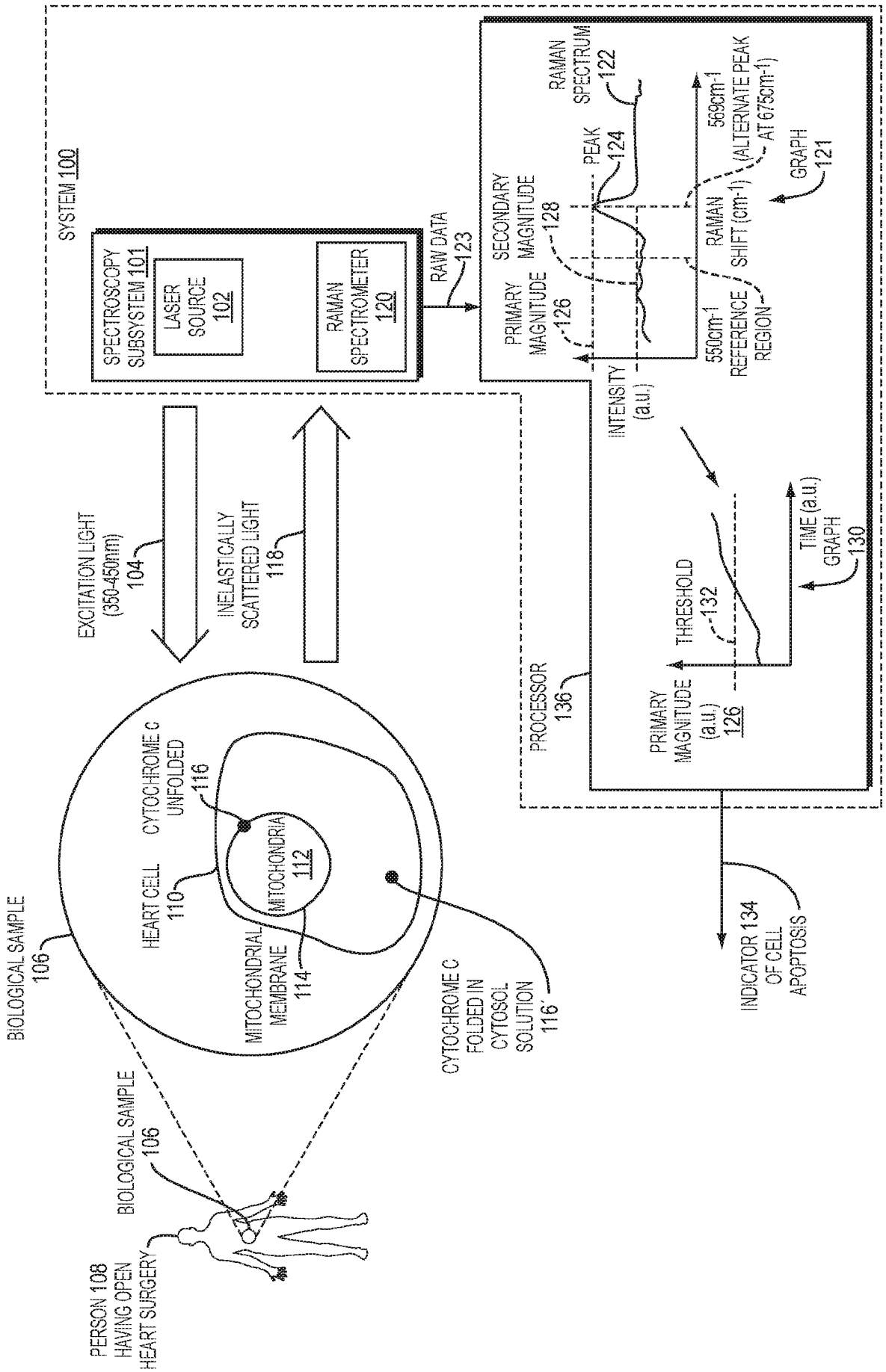
SYSTEM 100
SPECTROSCOPY SUBSYSTEM 101
LASER SOURCE 102
RAMAN SPECTROMETER 120
RAW DATA 123
EXCITATION LIGHT (350-450nm) 104
INELASTICALLY SCATTERED LIGHT 118
PROCESSOR 136
PRIMARY MAGNITUDE 126
SECONDARY MAGNITUDE 128
RAMAN SPECTRUM 122
PEAK 124
INTENSITY (a.u.)
550cm-1 REFERENCE REGION
RAMAN SHIFT (cm-1)
569cm-1 (ALTERNATE PEAK AT 675cm-1)
GRAPH 121
PRIMARY MAGNITUDE (a.u.) 126
THRESHOLD 132
TIME (a.u.) GRAPH 130
INDICATOR 134 OF CELL APOPTOSIS
BIOLOGICAL SAMPLE 106
HEART CELL 110
CYTOCHROME c UNFOLDED 116
MITOCHONDRIA 112
MITOCHONDRIAL MEMBRANE 114
CYTOCHROME C FOLDED IN CYTOSOL SOLUTION 116'
BIOLOGICAL SAMPLE 106
PERSON 108 HAVING OPEN HEART SURGERY

FIG. 1A

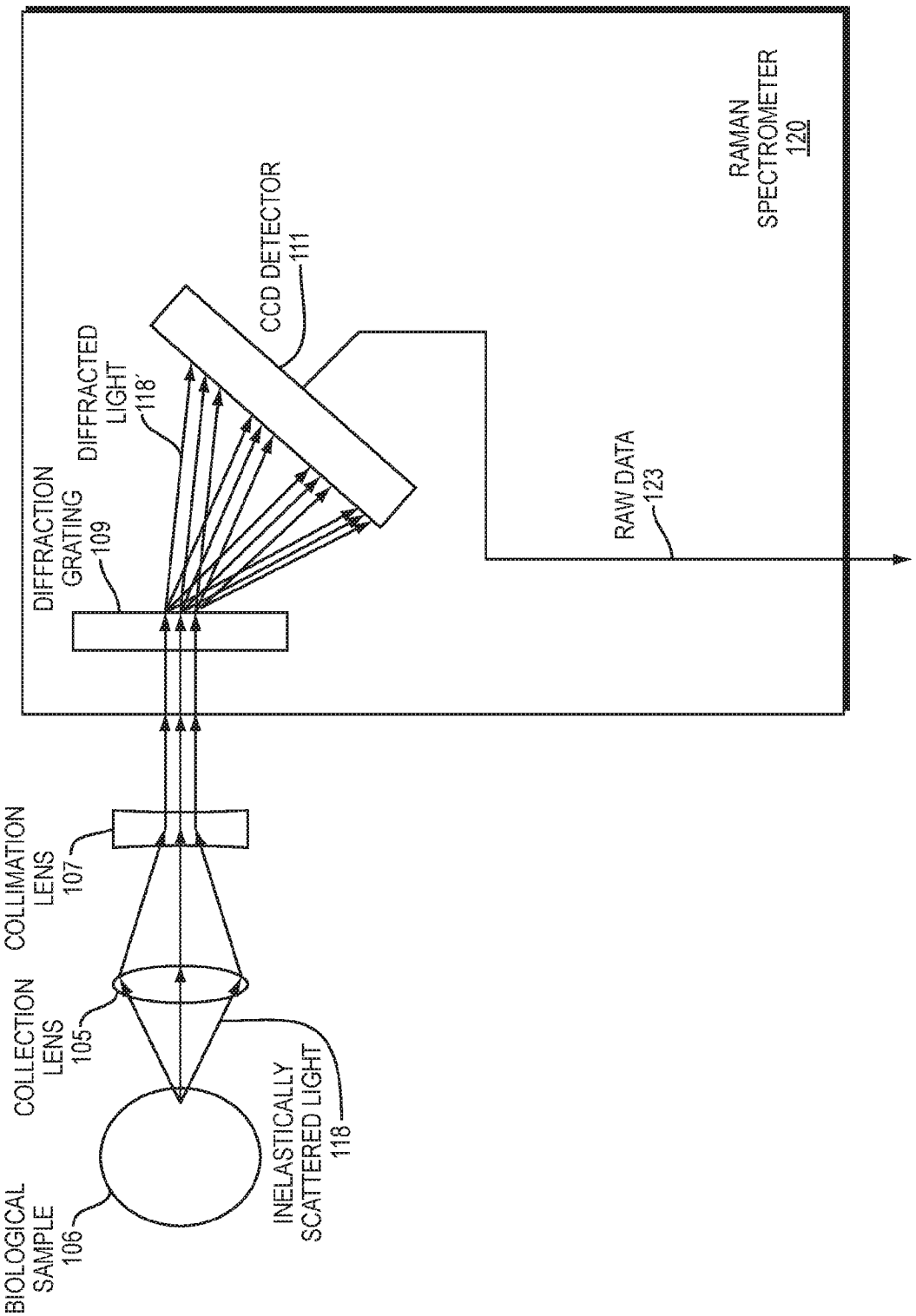
RAMAN SPECTROMETER 120
CCD DETECTOR 111
DIFFRACTED LIGHT 118'
DIFFRACTION GRATING 109
RAW DATA 123
COLLIMATION LENS 107
COLLECTION LENS 105
INELASTICALLY SCATTERED LIGHT 118
BIOLOGICAL SAMPLE 106

FIG. 1B

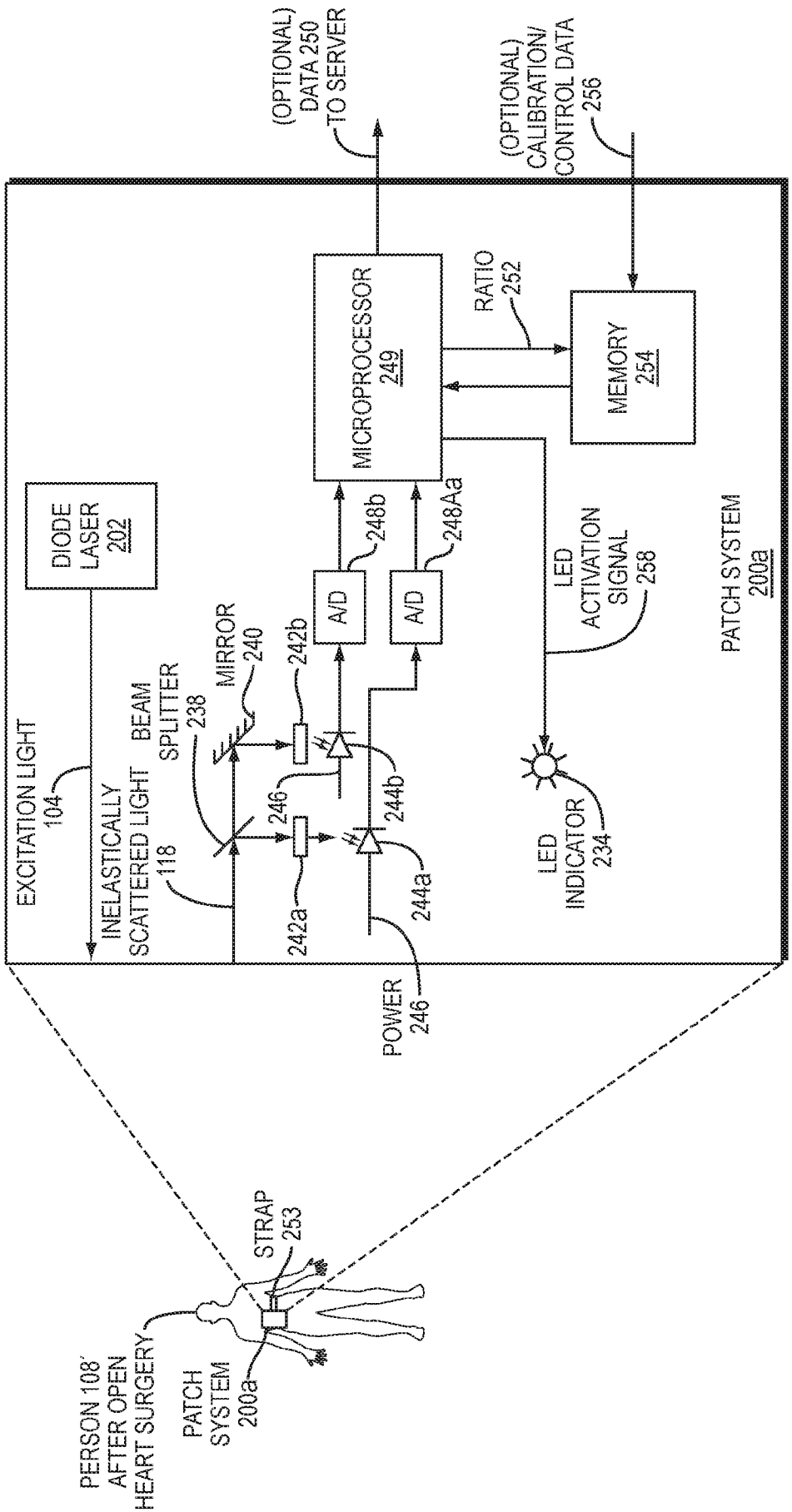
(OPTIONAL) DATA 250 TO SERVER
(OPTIONAL) CALIBRATION/ CONTROL DATA 256
MICROPROCESSOR 249
RATIO 252
MEMORY 254
DIODE LASER 202
A/D
248b
248Aa
LED ACTIVATION SIGNAL 258
PATCH SYSTEM 200a
MIRROR 240
242b
BEAM SPLITTER 238
EXCITATION LIGHT 104
INELASTICALLY SCATTERED LIGHT 118
246
244b
242a
244a
LED INDICATOR 234
POWER 246
STRAP 253
PERSON 108' AFTER OPEN HEART SURGERY
PATCH SYSTEM 200a

FIG. 2A

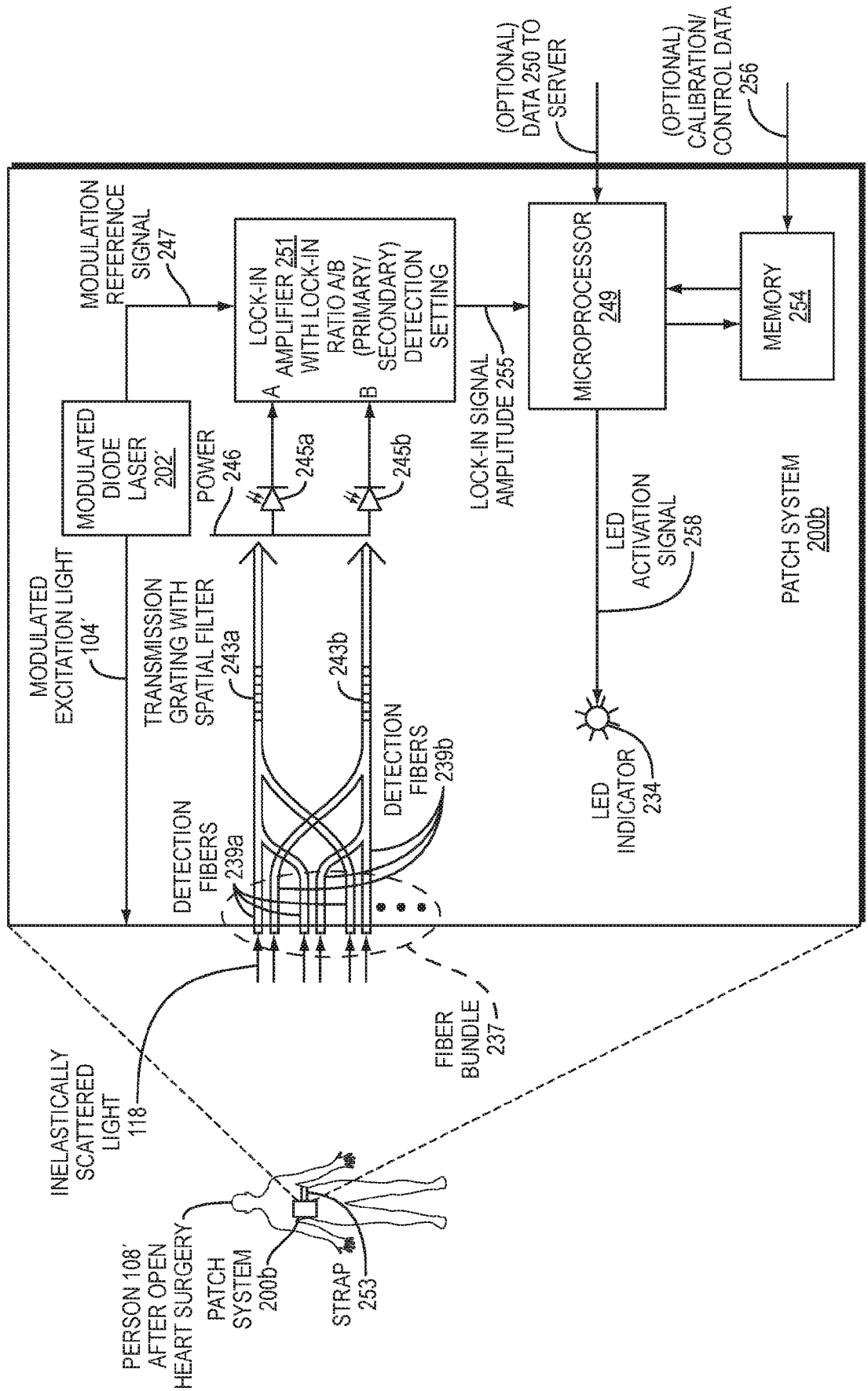
(OPTIONAL) DATA 250 TO SERVER
(OPTIONAL) CALIBRATION/ CONTROL DATA 256
MODULATION REFERENCE SIGNAL 247
LOCK-IN AMPLIFIER 251 WITH LOCK-IN RATIO A/B (PRIMARY/ SECONDARY) DETECTION SETTING
A
B
MICROPROCESSOR 249
MEMORY 254
MODULATED DIODE LASER 202'
POWER 246
245a
245b
LOCK-IN SIGNAL AMPLITUDE 255
LED ACTIVATION SIGNAL 258
PATCH SYSTEM 200b
MODULATED EXCITATION LIGHT 104'
TRANSMISSION GRATING WITH SPATIAL FILTER
243a
243b
DETECTION FIBERS 239a
DETECTION FIBERS 239b
LED INDICATOR 234
FIBER BUNDLE 237
INELASTICALLY SCATTERED LIGHT 118
PERSON 108' AFTER OPEN HEART SURGERY
PATCH SYSTEM 200b
STRAP 253

FIG. 2B

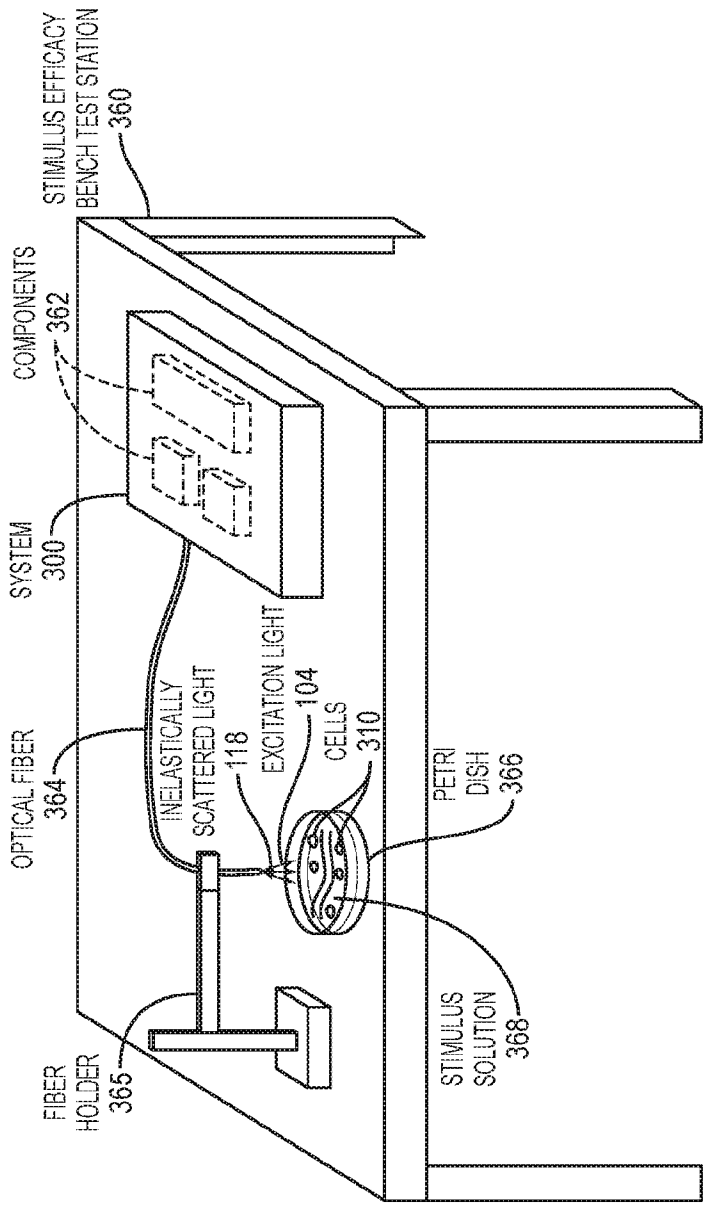
STIMULUS EFFICACY BENCH TEST STATION 360
COMPONENTS 362
SYSTEM 300
OPTICAL FIBER 364
INELASTICALLY SCATTERED LIGHT 118
EXCITATION LIGHT 104
CELLS 310
PETRI DISH 366
FIBER HOLDER 365
STIMULUS SOLUTION 368

FIG. 3

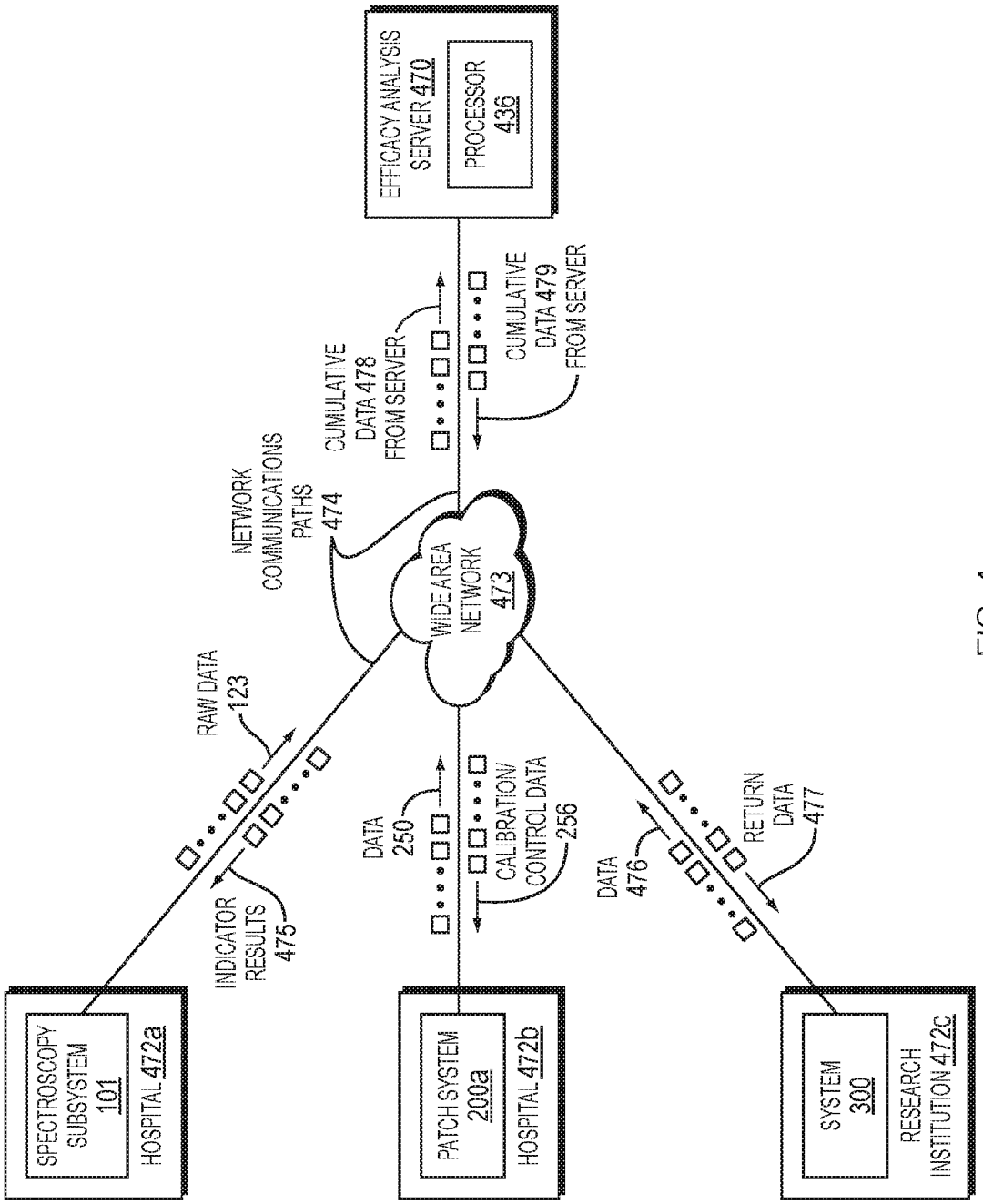
EFFICACY ANALYSIS SERVER 470
PROCESSOR 436
CUMULATIVE DATA 479 FROM SERVER
CUMULATIVE DATA 478 FROM SERVER
NETWORK COMMUNICATIONS PATHS 474
WIDE AREA NETWORK 473
RAW DATA 123
INDICATOR RESULTS 475
DATA 250
CALIBRATION/ CONTROL DATA 256
DATA 476
RETURN DATA 477
SPECTROSCOPY SUBSYSTEM 101
HOSPITAL 472a
PATCH SYSTEM 200a
HOSPITAL 472b
SYSTEM 300
RESEARCH INSTITUTION 472c

FIG. 4

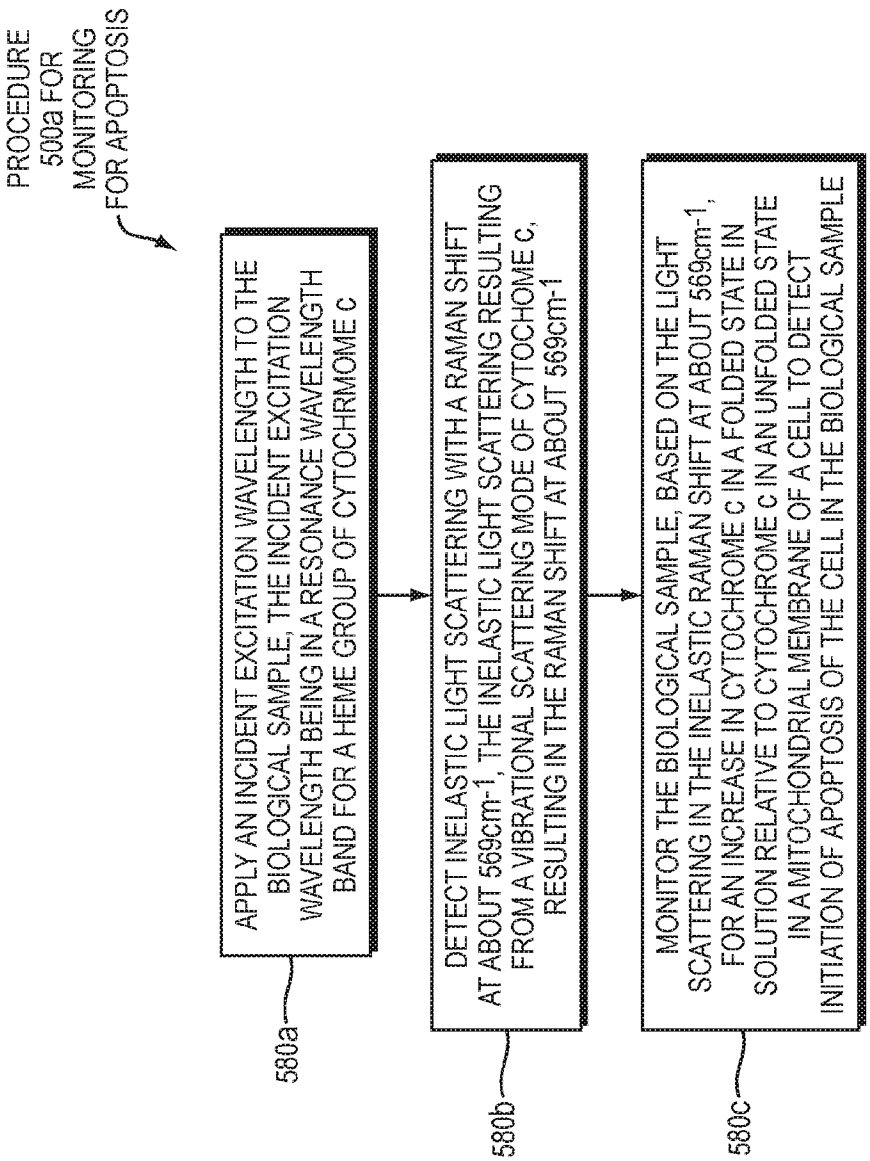
PROCEDURE 500a FOR MONITORING FOR APOPTOSIS
APPLY AN INCIDENT EXCITATION WAVELENGTH TO THE BIOLOGICAL SAMPLE, THE INCIDENT EXCITATION WAVELENGTH BEING IN A RESONANCE WAVELENGTH BAND FOR A HEME GROUP OF CYTOCHRMOME c
580a
DETECT INELASTIC LIGHT SCATTERING WITH A RAMAN SHIFT AT ABOUT 569cm-1, THE INELASTIC LIGHT SCATTERING RESULTING FROM A VIBRATIONAL SCATTERING MODE OF CYTOCHOME c, RESULTING IN THE RAMAN SHIFT AT ABOUT 569cm-1
580b
MONITOR THE BIOLOGICAL SAMPLE, BASED ON THE LIGHT SCATTERING IN THE INELASTIC RAMAN SHIFT AT ABOUT 569cm-1, FOR AN INCREASE IN CYTOCHROME c IN A FOLDED STATE IN SOLUTION RELATIVE TO CYTOCHROME c IN AN UNFOLDED STATE IN A MITOCHONDRIAL MEMBRANE OF A CELL TO DETECT INITIATION OF APOPTOSIS OF THE CELL IN THE BIOLOGICAL SAMPLE
580c

FIG. 5A

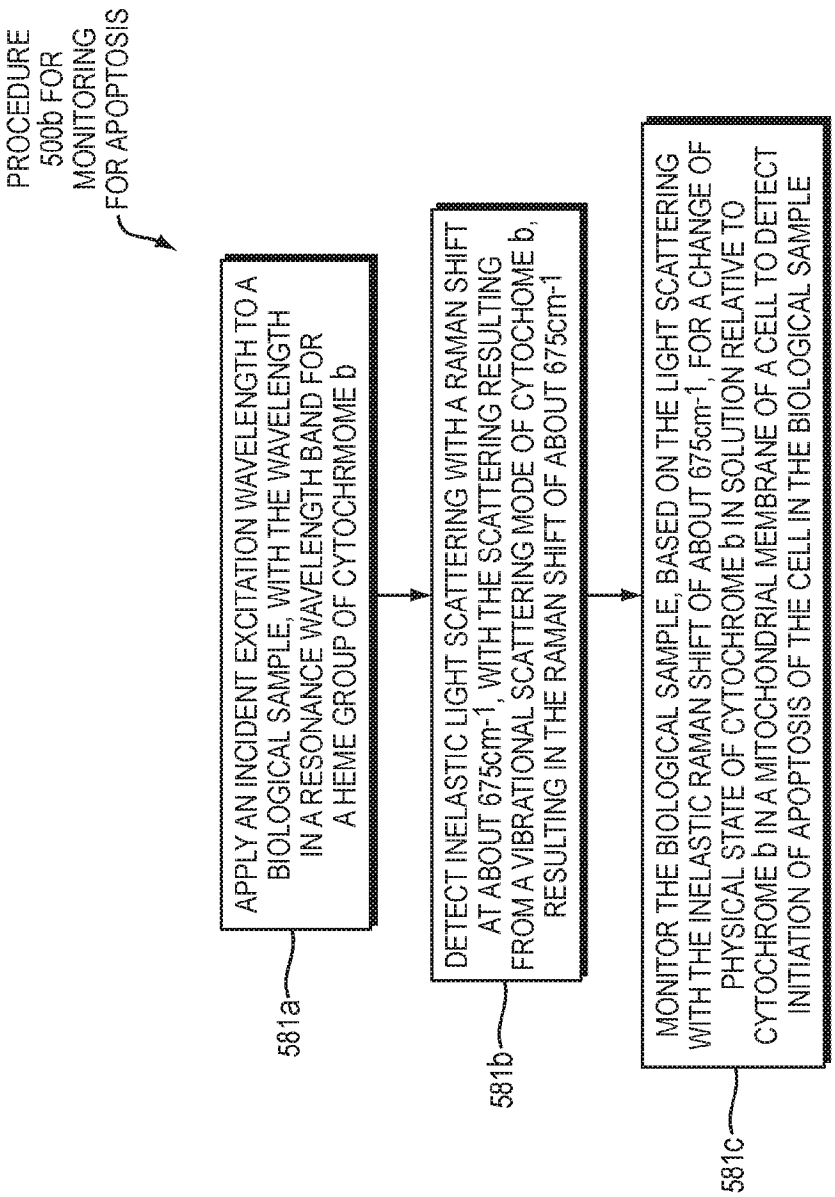
PROCEDURE 500b FOR MONITORING FOR APOPTOSIS
APPLY AN INCIDENT EXCITATION WAVELENGTH TO A BIOLOGICAL SAMPLE, WITH THE WAVELENGTH IN A RESONANCE WAVELENGTH BAND FOR A HEME GROUP OF CYTOCHRMOME b
581a
DETECT INELASTIC LIGHT SCATTERING WITH A RAMAN SHIFT AT ABOUT 675cm-1, WITH THE SCATTERING RESULTING FROM A VIBRATIONAL SCATTERING MODE OF CYTOCHOME b, RESULTING IN THE RAMAN SHIFT OF ABOUT 675cm-1
581b
MONITOR THE BIOLOGICAL SAMPLE, BASED ON THE LIGHT SCATTERING WITH THE INELASTIC RAMAN SHIFT OF ABOUT 675cm-1, FOR A CHANGE OF PHYSICAL STATE OF CYTOCHROME b IN SOLUTION RELATIVE TO CYTOCHROME b IN A MITOCHONDRIAL MEMBRANE OF A CELL TO DETECT INITIATION OF APOPTOSIS OF THE CELL IN THE BIOLOGICAL SAMPLE
581c

FIG. 5B

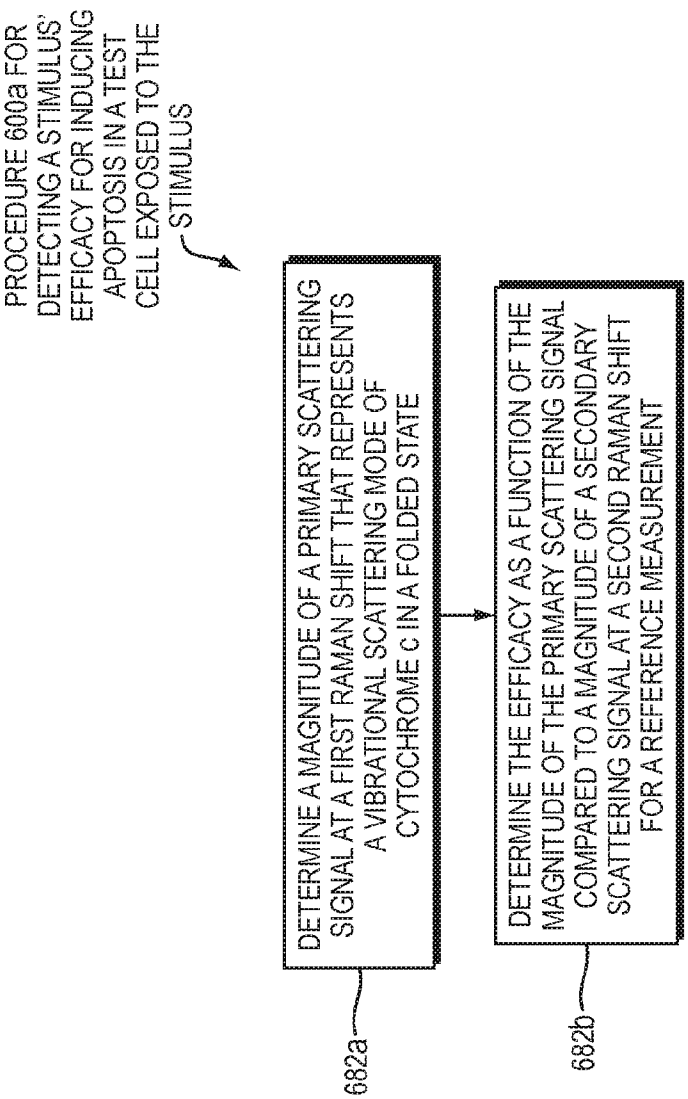
PROCEDURE 600a FOR DETECTING A STIMULUS' EFFICACY FOR INDUCING APOPTOSIS IN A TEST CELL EXPOSED TO THE STIMULUS
DETERMINE A MAGNITUDE OF A PRIMARY SCATTERING SIGNAL AT A FIRST RAMAN SHIFT THAT REPRESENTS A VIBRATIONAL SCATTERING MODE OF CYTOCHROME c IN A FOLDED STATE
682a
DETERMINE THE EFFICACY AS A FUNCTION OF THE MAGNITUDE OF THE PRIMARY SCATTERING SIGNAL COMPARED TO A MAGNITUDE OF A SECONDARY SCATTERING SIGNAL AT A SECOND RAMAN SHIFT FOR A REFERENCE MEASUREMENT
682b

FIG. 6A

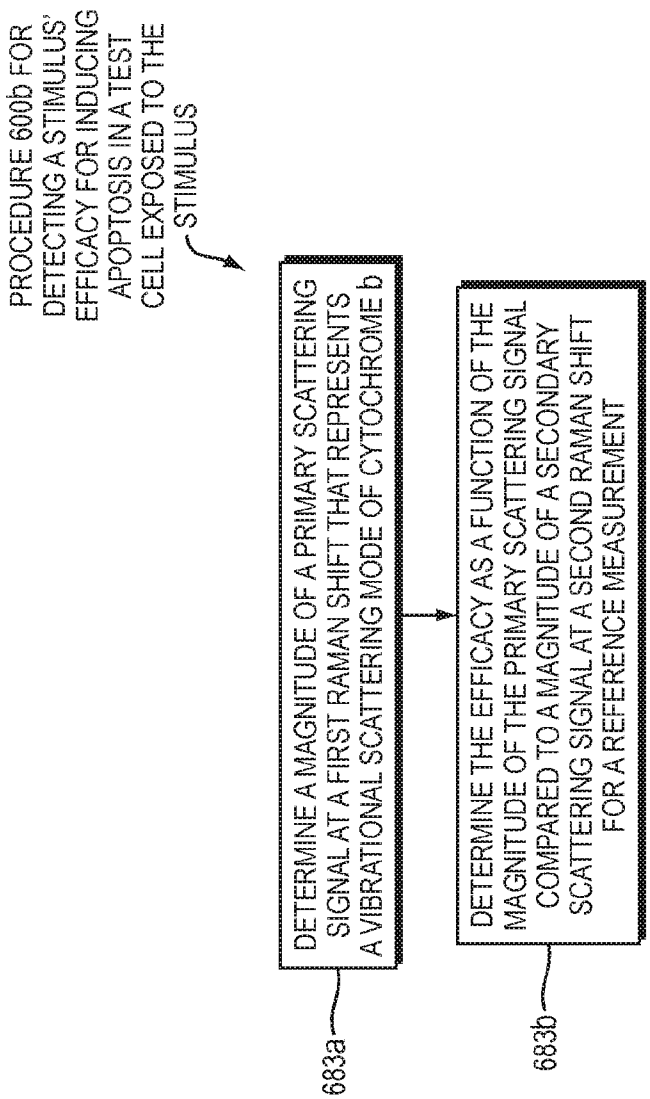
PROCEDURE 600b FOR DETECTING A STIMULUS' EFFICACY FOR INDUCING APOPTOSIS IN A TEST CELL EXPOSED TO THE STIMULUS
DETERMINE A MAGNITUDE OF A PRIMARY SCATTERING SIGNAL AT A FIRST RAMAN SHIFT THAT REPRESENTS A VIBRATIONAL SCATTERING MODE OF CYTOCHROME b
683a
DETERMINE THE EFFICACY AS A FUNCTION OF THE MAGNITUDE OF THE PRIMARY SCATTERING SIGNAL COMPARED TO A MAGNITUDE OF A SECONDARY SCATTERING SIGNAL AT A SECOND RAMAN SHIFT FOR A REFERENCE MEASUREMENT
683b

FIG. 6B

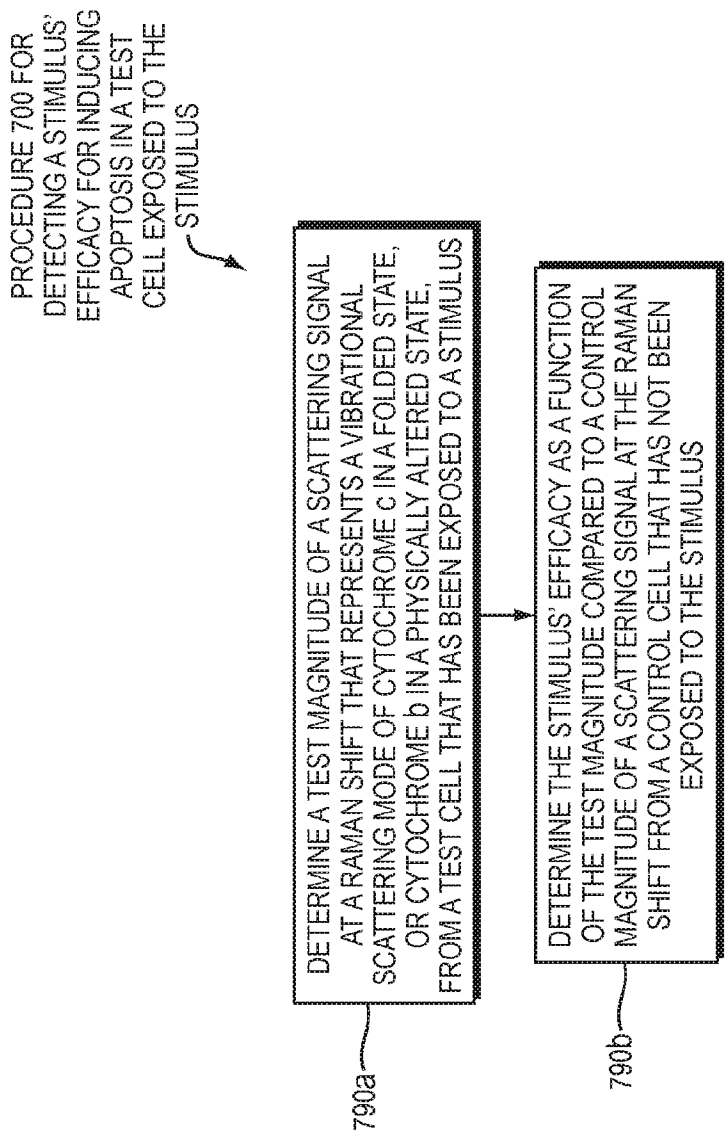
PROCEDURE 700 FOR DETECTING A STIMULUS' EFFICACY FOR INDUCING APOPTOSIS IN A TEST CELL EXPOSED TO THE STIMULUS
DETERMINE A TEST MAGNITUDE OF A SCATTERING SIGNAL AT A RAMAN SHIFT THAT REPRESENTS A VIBRATIONAL SCATTERING MODE OF CYTOCHROME c IN A FOLDED STATE, OR CYTOCHROME b IN A PHYSICALLY ALTERED STATE, FROM A TEST CELL THAT HAS BEEN EXPOSED TO A STIMULUS
790a
DETERMINE THE STIMULUS' EFFICACY AS A FUNCTION OF THE TEST MAGNITUDE COMPARED TO A CONTROL MAGNITUDE OF A SCATTERING SIGNAL AT THE RAMAN SHIFT FROM A CONTROL CELL THAT HAS NOT BEEN EXPOSED TO THE STIMULUS
790b

FIG. 7

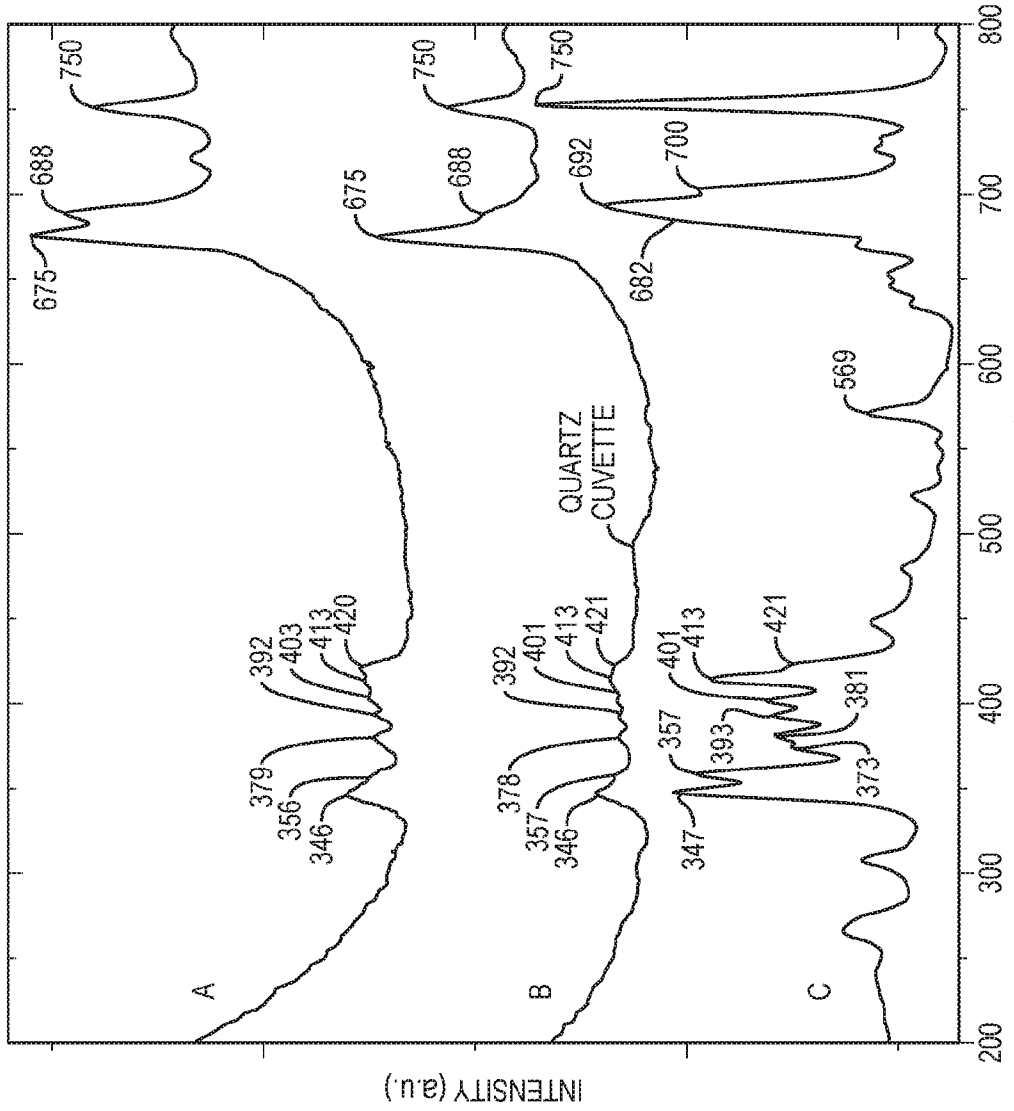
INTENSITY (a.u.)
RAMAN SHIFT (cm-1)
200
300
400
500
600
700
800
A
B
C
QUARTZ CUVETTE
675
688
750
392
403
413
420
379
356
346
675
688
750
392
401
413
421
378
357
346
682
692
700
750
569
401
413
421
357
393
381
347
373

FIG. 8A

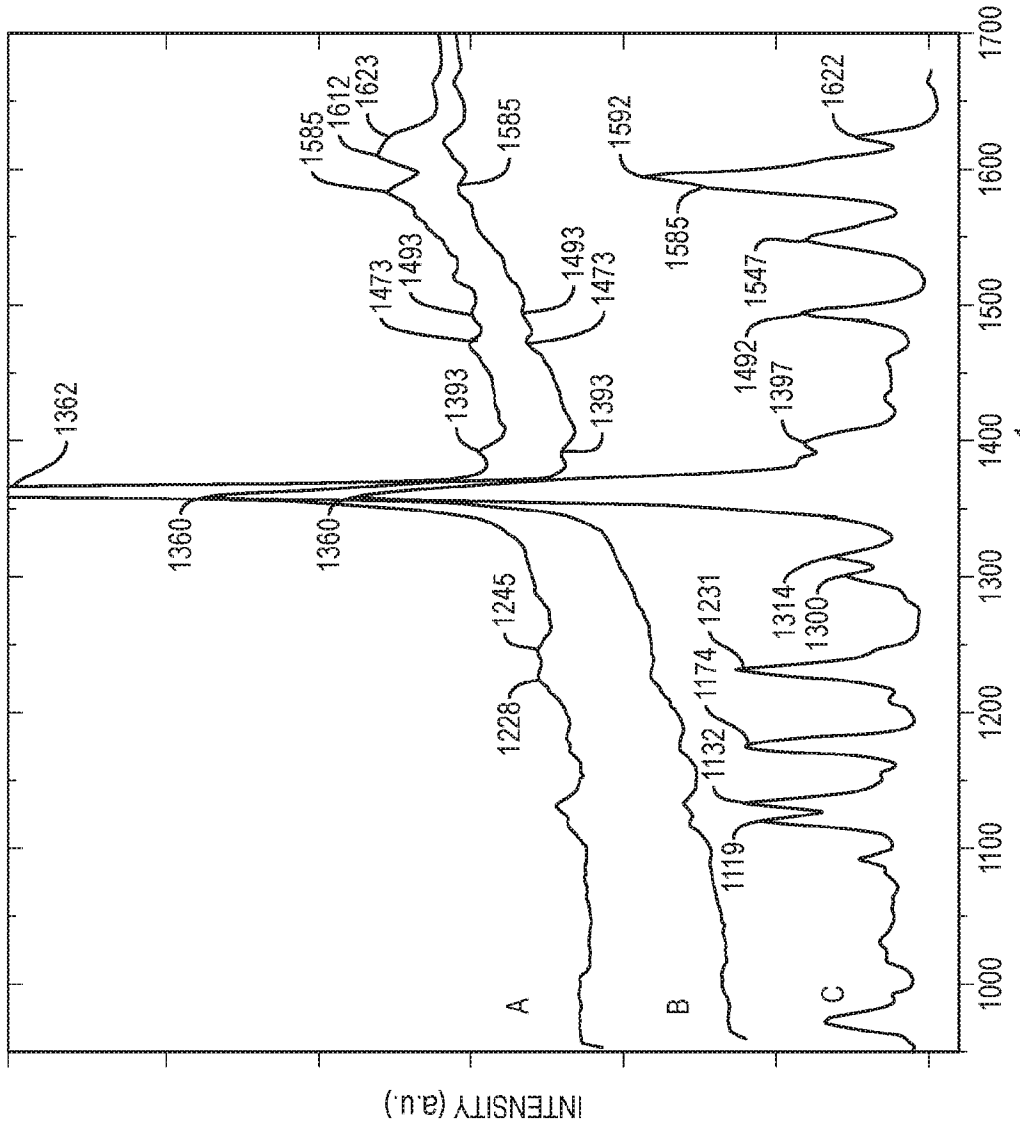
INTENSITY (a.u.)
RAMAN SHIFT (cm-1)
1000
1100
1200
1300
1400
1500
1600
1700
A
B
C
1362
1360
1360
1245
1228
1231
1174
1132
1119
1314
1300
1393
1393
1473
1493
1493
1473
1585
1612
1623
1585
1592
1585
1492
1547
1397
1622

FIG. 8B

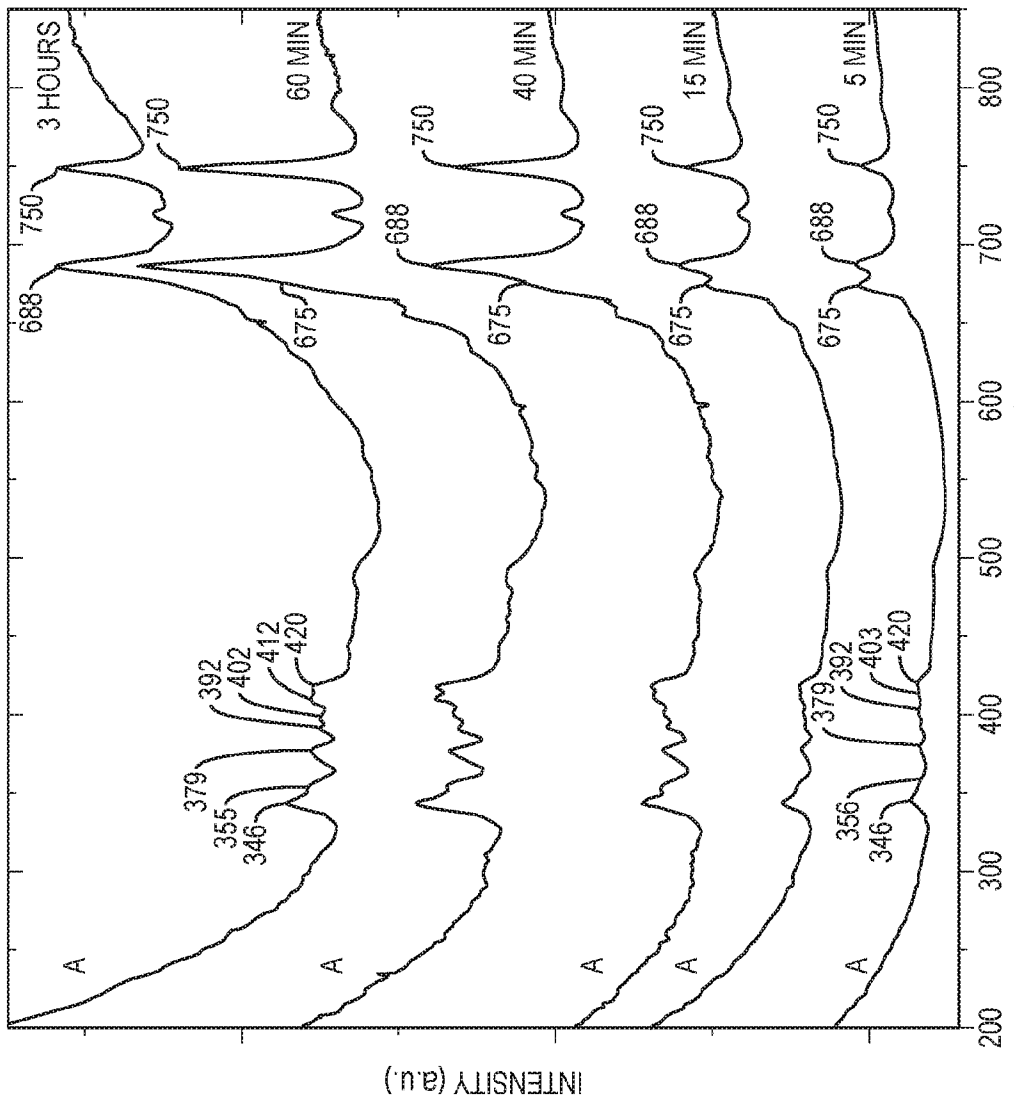
3 HOURS
60 MIN
40 MIN
15 MIN
5 MIN
688
750
675
379
355
346
392
402
412
420
403
356
A
INTENSITY (a.u.)
RAMAN SHIFT (cm-1)
200
300
400
500
600
700
800

FIG. 9A

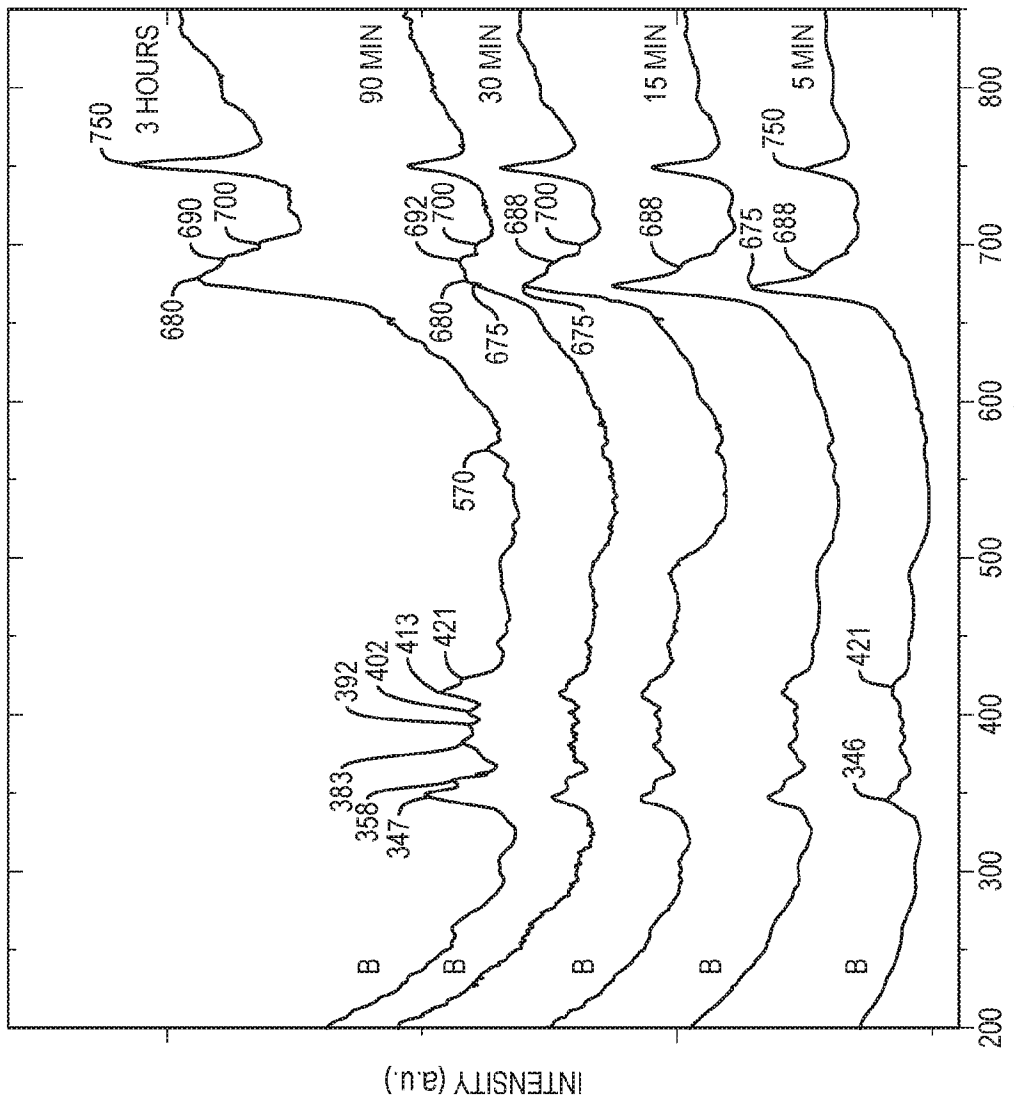
3 HOURS
90 MIN
30 MIN
15 MIN
5 MIN
750
690
700
680
692
688
675
570
392
402
413
421
383
358
347
346
B
INTENSITY (a.u.)
RAMAN SHIFT (cm-1)
200
300
400
500
600
700
800

FIG. 9B

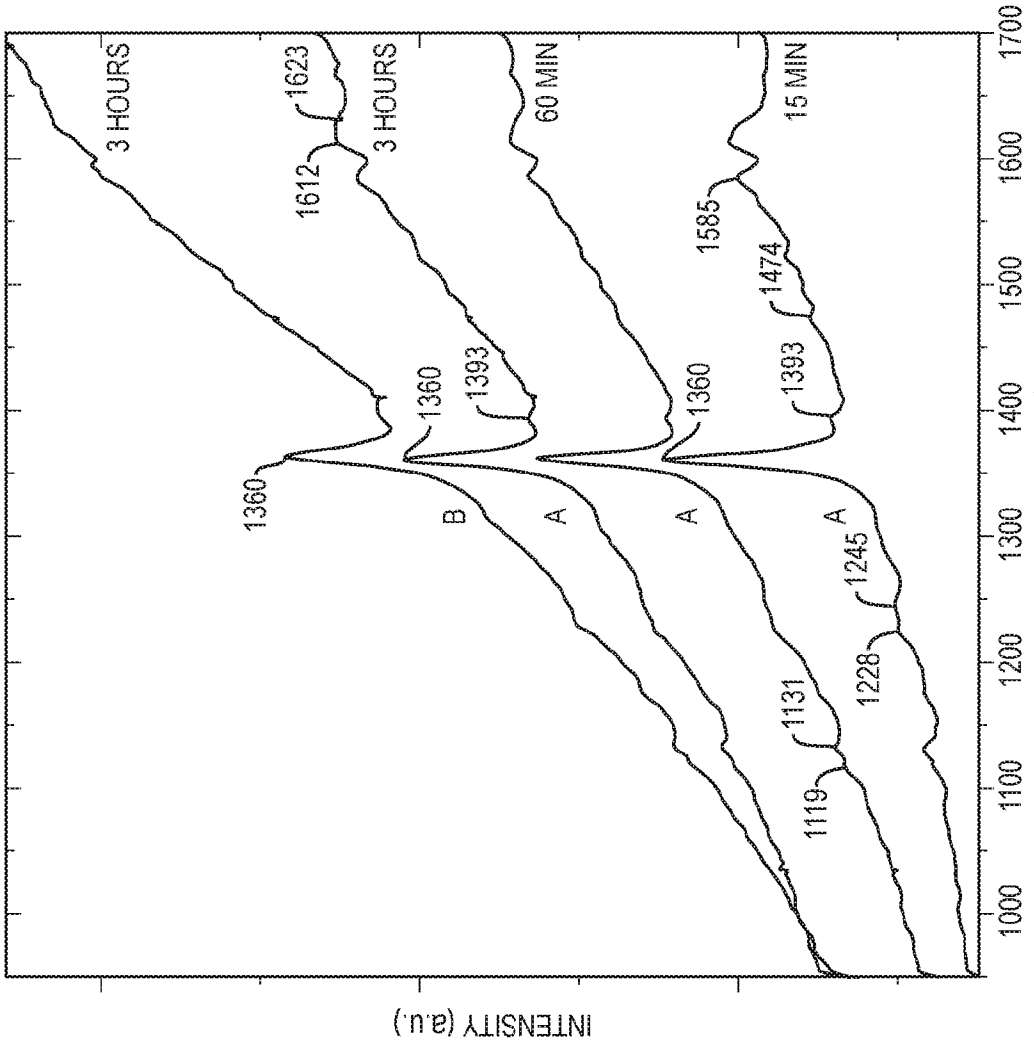
3 HOURS
1623
1612
3 HOURS
60 MIN
15 MIN
1585
1474
1360
1393
1360
1360
1393
B
A
A
A
1245
1228
1131
1119
INTENSITY (a.u.)
1000
1100
1200
1300
1400
1500
1600
1700
RAMAN SHIFT (cm-1)

FIG. 10

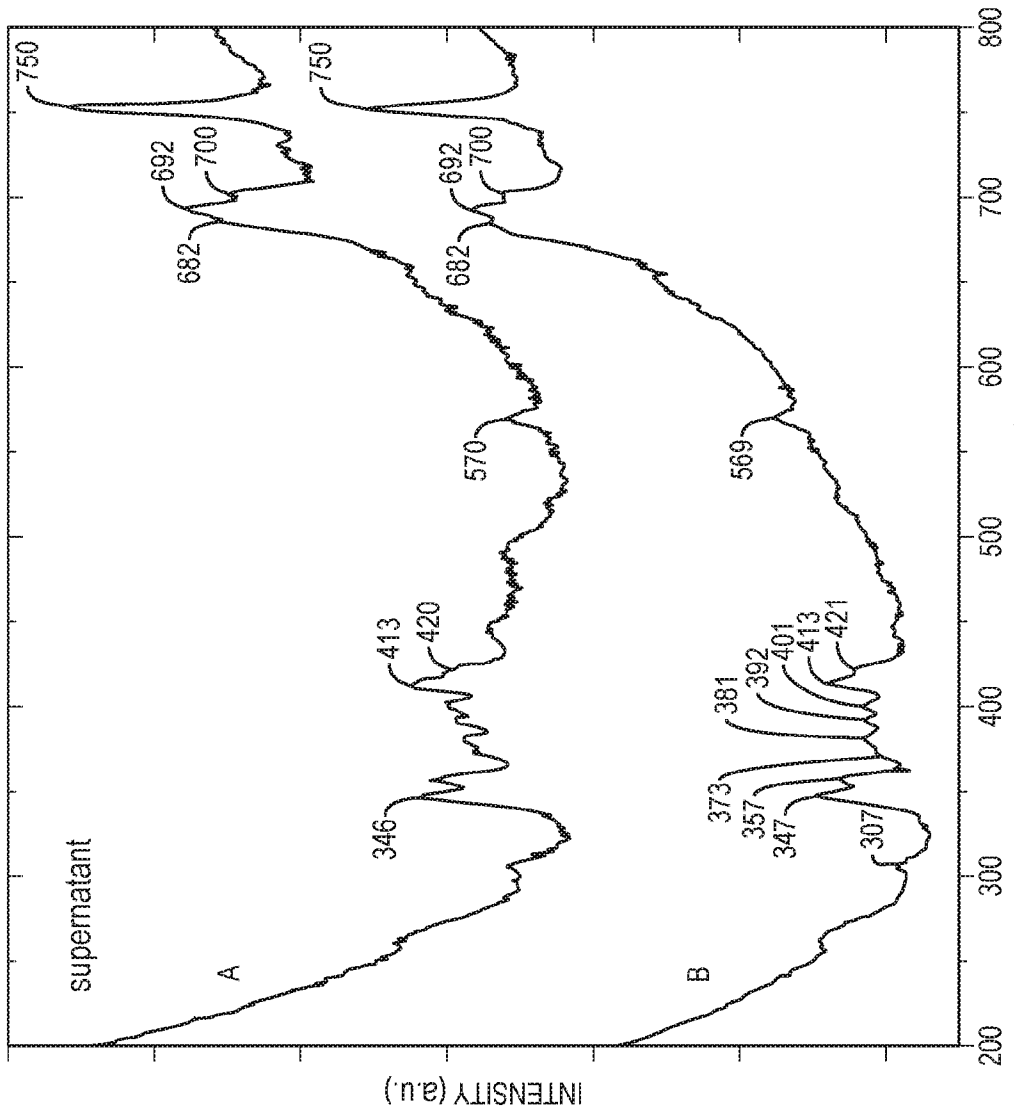
supernatant
A
B
750
692
700
682
570
413
420
346
750
692
700
682
569
381
392
401
413
421
373
357
347
307
200
300
400
500
600
700
800
RAMAN SHIFT (cm-1)
INTENSITY (a.u.)

FIG. 11A

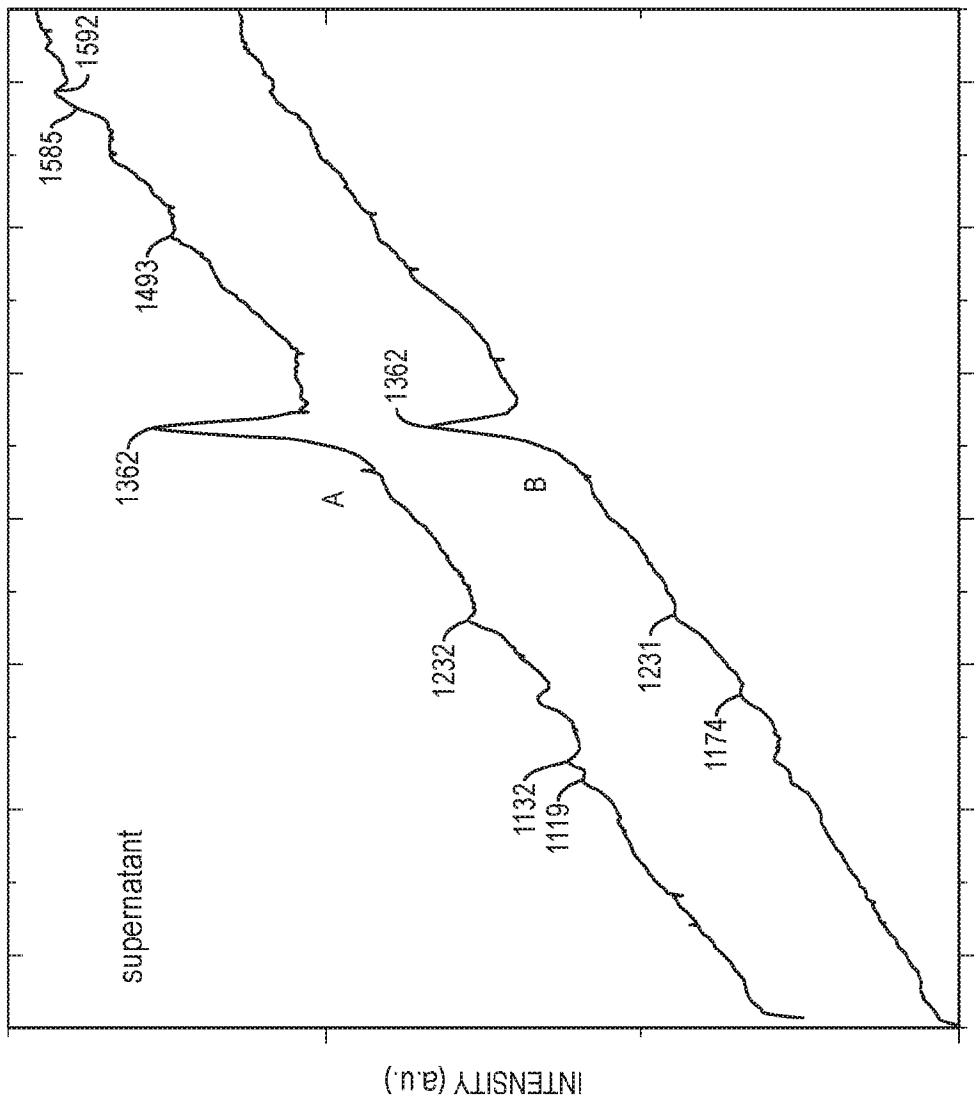
supernatant
A
B
1585
1592
1493
1362
1362
1232
1132
1119
1231
1174
1000
1100
1200
1300
1400
1500
1600
RAMAN SHIFT (cm-1)
INTENSITY (a.u.)

FIG. 11B

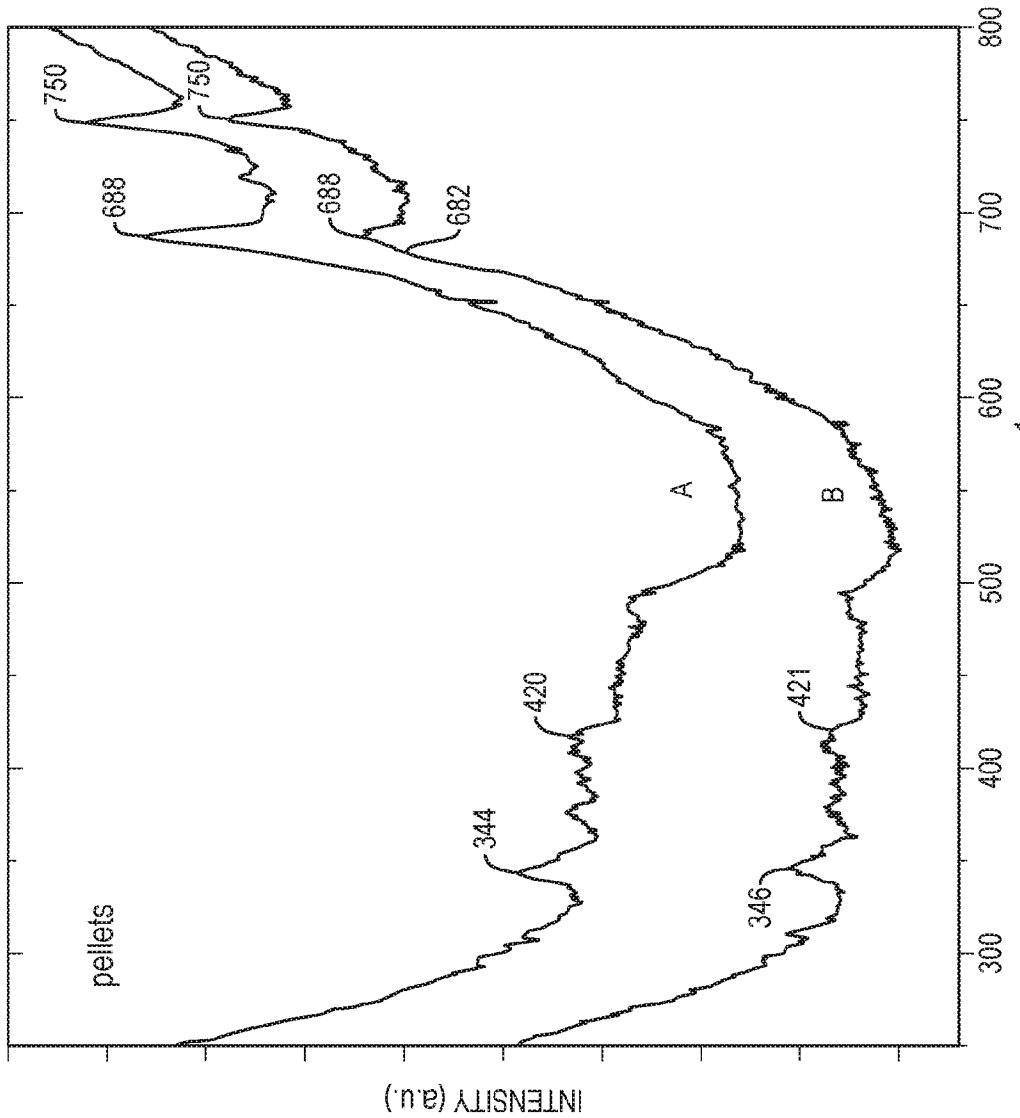
pellets
750
750
688
688
682
A
B
420
344
421
346
INTENSITY (a.u.)
300
400
500
600
700
800
RAMAN SHIFT (cm-1)

FIG. 12A

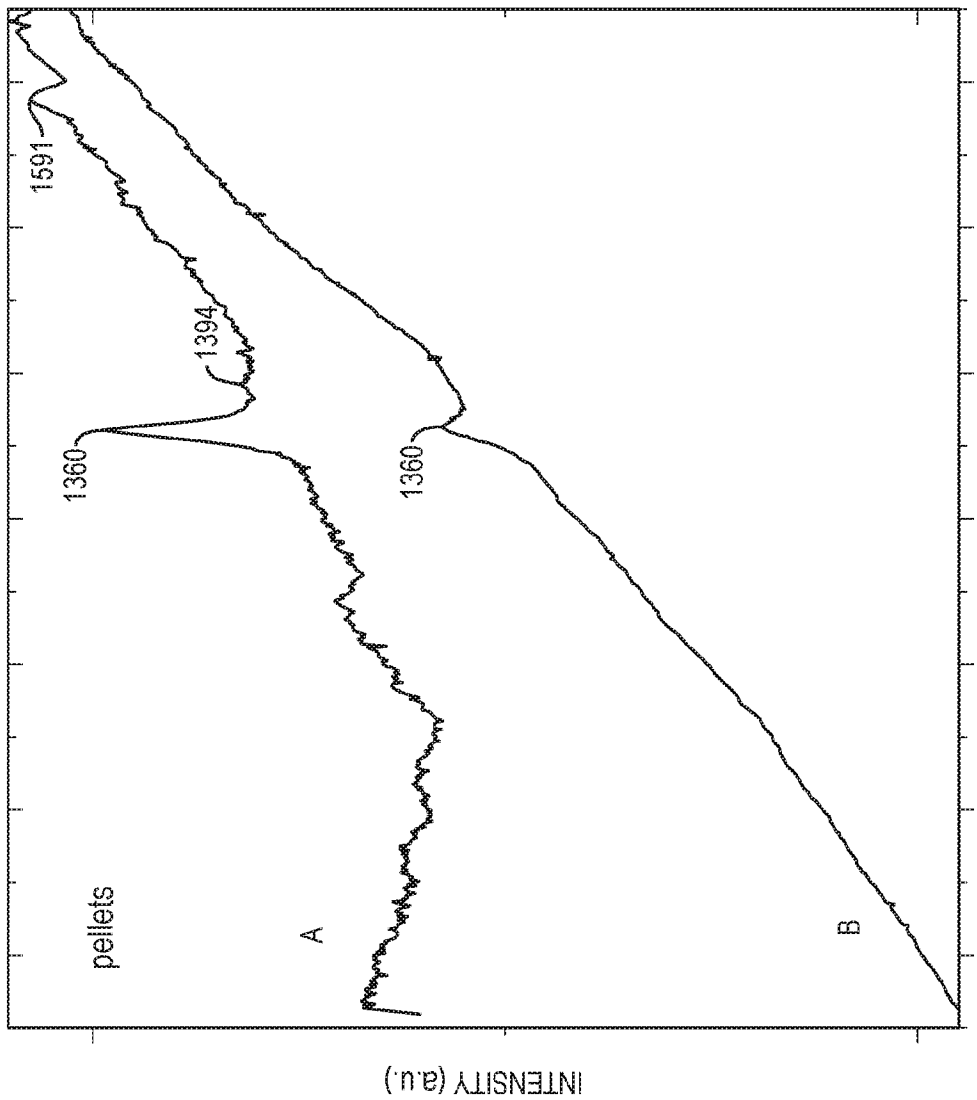
pellets
A
B
1591
1394
1360
1360
1000
1100
1200
1300
1400
1500
1600
RAMAN SHIFT (cm-1)
INTENSITY (a.u.)

FIG. 12B

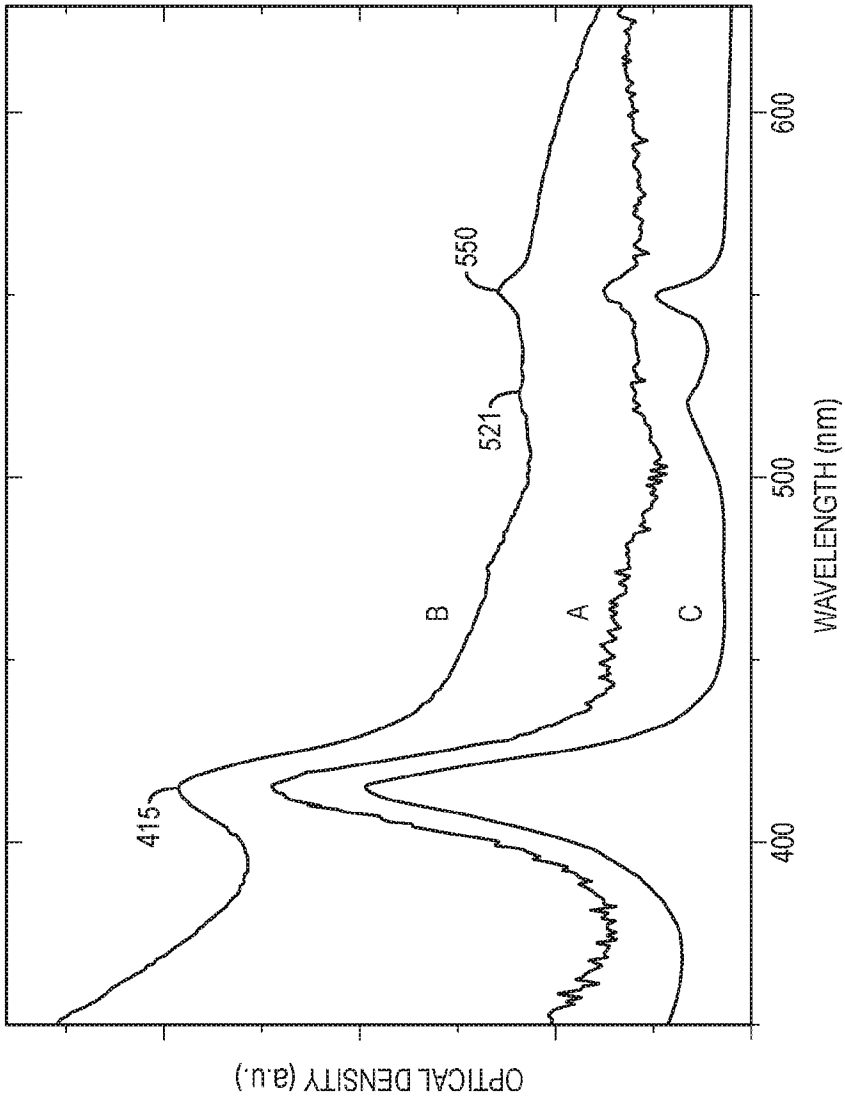

FIG. 13

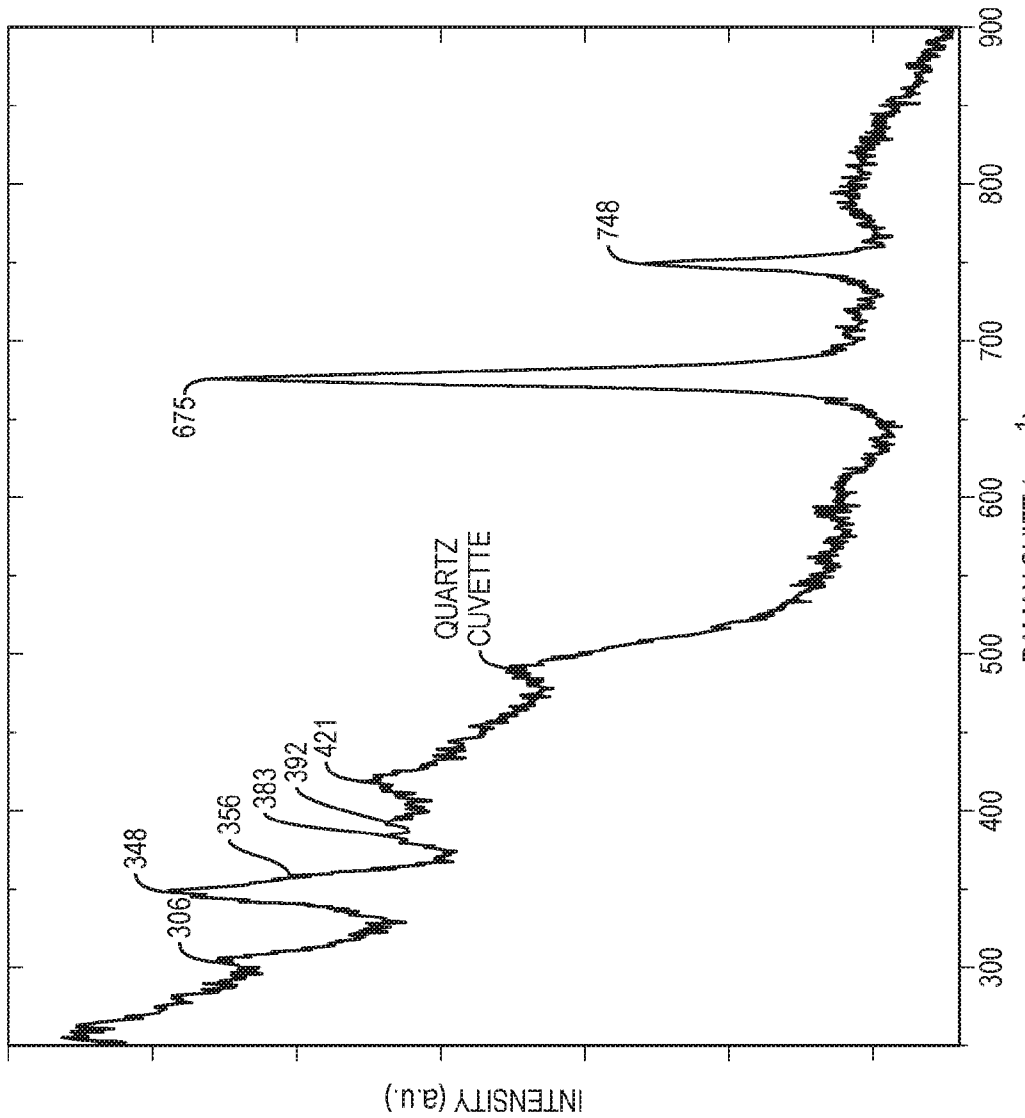
INTENSITY (a.u.)
RAMAN SHIFT (cm-1)
300
400
500
600
700
800
900
348
306
356
383
392
421
QUARTZ
CUVETTE
675
748

FIG. 14

INTERNATIONAL SEARCH REPORT

International application No
PCT/US2015/063801

A. CLASSIFICATION OF SUBJECT MATTER
INV. G01N21/65 A61B5/00 G01N33/50
ADD.

According to International Patent Classification (IPC) or to both national classification and IPC

B. FIELDS SEARCHED

Minimum documentation searched (classification system followed by classification symbols)
G01N A61B

Documentation searched other than minimum documentation to the extent that such documents are included in the fields searched

Electronic data base consulted during the international search (name of data base and, where practicable, search terms used)
EPO-Internal, WPI Data

C. DOCUMENTS CONSIDERED TO BE RELEVANT

Category*	Citation of document, with indication, where appropriate, of the relevant passages	Relevant to claim No.
Y	JANICE L. PANZA ET AL: "<title>Raman spectroscopy and Raman chemical imaging of apoptotic cells</title>", PROCEEDINGS SPIE, vol. 6441, 8 February 2007 (2007-02-08), page 644108, XP055259734, ISSN: 0277-786X, DOI: 10.1117/12.701219 Sections; abstract; figures Sections 2.1, 3.2 and 4. -----	1
Y	DE 10 2012 005583 A1 (OPSOLUTION GMBH [DE]) 29 May 2013 (2013-05-29) paragraphs [0013] - [0014], [0030], [0035], [0049] - [0051], [0055] - [0056], [0061]; figures ----- -/--	1

[X] Further documents are listed in the continuation of Box C.

[X] See patent family annex.

* Special categories of cited documents :

"A" document defining the general state of the art which is not considered to be of particular relevance

"E" earlier application or patent but published on or after the international filing date

"L" document which may throw doubts on priority claim(s) or which is cited to establish the publication date of another citation or other special reason (as specified)

"O" document referring to an oral disclosure, use, exhibition or other means

"P" document published prior to the international filing date but later than the priority date claimed

"T" later document published after the international filing date or priority date and not in conflict with the application but cited to understand the principle or theory underlying the invention

"X" document of particular relevance; the claimed invention cannot be considered novel or cannot be considered to involve an inventive step when the document is taken alone

"Y" document of particular relevance; the claimed invention cannot be considered to involve an inventive step when the document is combined with one or more other such documents, such combination being obvious to a person skilled in the art

"&" document member of the same patent family

Date of the actual completion of the international search	Date of mailing of the international search report
31 May 2016	07/06/2016

Name and mailing address of the ISA/	Authorized officer
European Patent Office, P.B. 5818 Patentlaan 2 NL - 2280 HV Rijswijk Tel. (+31-70) 340-2040, Fax: (+31-70) 340-3016	Riblet, Philippe

INTERNATIONAL SEARCH REPORT

International application No
PCT/US2015/063801

C(Continuation). DOCUMENTS CONSIDERED TO BE RELEVANT

Category*	Citation of document, with indication, where appropriate, of the relevant passages	Relevant to claim No.
Y	JP 2002 085385 A (HONDA SADAKO) 26 March 2002 (2002-03-26) abstract; figures	1
A	WO 2010/144081 A1 (UNIV UTAH RES FOUND [US]; MCCLANE ROBERT W [US]; BENTZ BRANDON G [US]) 16 December 2010 (2010-12-16) paragraphs [0001], [0002], [0004], [0007], [0011], [0014], [0030], [0036], [0051]; figures	1
X	SVITLANA BEREZHNA ET AL: "Resonance Raman Investigations of Cytochrome c Conformational Change upon Interaction with the Membranes of Intact and Ca 2+ -Exposed Mitochondria +", BIOCHEMISTRY, vol. 42, no. 20, 1 May 2003 (2003-05-01), pages 6149-6158, XP055274023, US ISSN: 0006-2960, DOI: 10.1021/bi027387y	5,6,9, 11,13, 14, 17-21, 24-28
Y	the whole document	2-4,7,8, 10,12, 23,32-35
X	M. OKADA ET AL: "Label-free Raman observation of cytochrome c dynamics during apoptosis", PROCEEDINGS OF THE NATIONAL ACADEMY OF SCIENCES, vol. 109, no. 1, 3 January 2012 (2012-01-03), pages 28-32, XP055274015, US ISSN: 0027-8424, DOI: 10.1073/pnas.1107524108	4,15, 29-31
Y	the whole document	2,3,7,8, 10,12, 16,22, 23,32-35
Y	SALEHI HAMIDEH ET AL: "Confocal Raman data analysis enables identifying apoptosis of MCF-7 cells caused by anticancer drug paclitaxel", JOURNAL OF BIOMEDICAL OPTICS, S P I E - INTERNATIONAL SOCIETY FOR OPTICAL ENGINEERING, US, vol. 18, no. 5, 1 May 2013 (2013-05-01), page 56010, XP060024161, ISSN: 1083-3668, DOI: 10.1117/1.JBO.18.5.056010 [retrieved on 2013-05-09] Sections 1, 4.	2,3

-/--

INTERNATIONAL SEARCH REPORT

International application No
PCT/US2015/063801

C(Continuation). DOCUMENTS CONSIDERED TO BE RELEVANT

Category*	Citation of document, with indication, where appropriate, of the relevant passages	Relevant to claim No.
Y	FEDERICA SINIBALDI ET AL: "Extended cardiolipin anchorage to cytochrome c: a model for protein-mitochondrial membrane binding", JBIC JOURNAL OF BIOLOGICAL INORGANIC CHEMISTRY, SPRINGER, BERLIN, DE, vol. 15, no. 5, 18 March 2010 (2010-03-18) , pages 689-700, XP019854151, ISSN: 1432-1327 page 695; figures 6-7	2-4,10, 12,15, 16,22
Y	F. SINIBALDI ET AL: "ATP specifically drives refolding of non-native conformations of cytochrome c", PROTEIN SCIENCE, vol. 14, no. 4, 1 January 2005 (2005-01-01), pages 1049-1058, XP055259158, US ISSN: 0961-8368, DOI: 10.1110/ps.041069405 abstract page 1052, column 2	2-4,10, 12,15, 16,22

INTERNATIONAL SEARCH REPORT

International application No.
PCT/US2015/063801

Box No. II Observations where certain claims were found unsearchable (Continuation of item 2 of first sheet)

This international search report has not been established in respect of certain claims under Article 17(2)(a) for the following reasons:

1. ☐ Claims Nos.:
because they relate to subject matter not required to be searched by this Authority, namely:

2. ☐ Claims Nos.:
because they relate to parts of the international application that do not comply with the prescribed requirements to such an extent that no meaningful international search can be carried out, specifically:

3. ☐ Claims Nos.:
because they are dependent claims and are not drafted in accordance with the second and third sentences of Rule 6.4(a).

Box No. III Observations where unity of invention is lacking (Continuation of item 3 of first sheet)

This International Searching Authority found multiple inventions in this international application, as follows:

see additional sheet

1. ☒ As all required additional search fees were timely paid by the applicant, this international search report covers all searchable claims.

2. ☐ As all searchable claims could be searched without effort justifying an additional fees, this Authority did not invite payment of additional fees.

3. ☐ As only some of the required additional search fees were timely paid by the applicant, this international search report covers only those claims for which fees were paid, specifically claims Nos.:

4. ☐ No required additional search fees were timely paid by the applicant. Consequently, this international search report is restricted to the invention first mentioned in the claims; it is covered by claims Nos.:

Remark on Protest

☐ The additional search fees were accompanied by the applicant's protest and, where applicable, the payment of a protest fee.

☐ The additional search fees were accompanied by the applicant's protest but the applicable protest fee was not paid within the time limit specified in the invitation.

☒ No protest accompanied the payment of additional search fees.

FURTHER INFORMATION CONTINUED FROM PCT/ISA/ 210

This International Searching Authority found multiple (groups of) inventions in this international application, as follows:

1. claim: 1

relates to a system for monitoring for cell apoptosis using inelastic scattering (or Raman) spectroscopy.
The technical problem is how to perform such monitoring for in vivo biological sample.
The technical solution is to design the monitoring as a patch to be applied to a person comprising a laser source, a detector and a processor configured to monitor the state of the biological sample based on the light scattering.

---

2. claims: 2-35

relate to a system and method for monitoring or detecting for cell apoptosis in a biological sample using resonance Raman spectroscopy.The technical problem is how to monitor cell apoptosis at an early stage.The technical solution is to monitor cell apoptosis by following the appearance of the Raman peak at wavelength shift of about 569-570 cm-1 representative of out of plane heme vibrational modes of cytochrome c and/or the disappearance of the Raman peak at wavelength shift of about 675 cm-1 representative of a vibrational mode of cytochrome b in a mitochondrial membrane.

INTERNATIONAL SEARCH REPORT

Information on patent family members

International application No
PCT/US2015/063801

Patent document cited in search report	Publication date	Patent family member(s)	Publication date
DE 102012005583 A1	29-05-2013	DE 102012005583 A1	29-05-2013
		DE 112012003343 A5	04-12-2014
JP 2002085385 A	26-03-2002	NONE	
WO 2010144081 A1	16-12-2010	NONE	